SCHOOL OF ECONOMICS AND MANAGEMENT
FACULTY OF SOCIAL SCIENCES
AARHUS UNIVERSITY

CREATES
Center for Research in Econometric Analysis of Time Series

CREATES Research Paper 2011-19

Title: Fact or friction: Jumps at ultra high frequency

Kim Christensen, Roel Oomen and Mark Podolskij

School of Economics and Management
Aarhus University
Bartholins Allé 10, Building 1322, DK-8000 Aarhus C
Denmark

Fact or friction: Jumps at ultra high frequency

Kim Christensen Roel Oomen Mark Podolskij*

May, 2011

Abstract

In this paper, we demonstrate that jumps in financial asset prices are not nearly as common as generally thought, and that they account for only a very small proportion of total return variation. We base our investigation on an extensive set of ultra high-frequency equity and foreign exchange rate data recorded at milli-second precision, allowing us to view the price evolution at a microscopic level. We show that both in theory and practice, traditional measures of jump variation based on low-frequency tick data tend to spuriously attribute a burst of volatility to the jump component thereby severely overstating the true variation coming from jumps. Indeed, our estimates based on tick data suggest that the jump variation is an order of magnitude smaller. This finding has a number of important implications for asset pricing and risk management and we illustrate this with a delta hedging example of an option trader that is short gamma. Our econometric analysis is build around a pre-averaging theory that allows us to work at the highest available frequency, where the data are polluted by microstructure noise. We extend the theory in a number of directions important for jump estimation and testing. This also reveals that pre-averaging has a built-in robustness property to outliers in high-frequency data, and allows us to show that some of the few remaining jumps at tick frequency are in fact induced by data-cleaning routines aimed at removing the outliers.

JEL Classification: C10; C80.

Keywords: jump variation; high-frequency data; market microstructure noise; pre-averaging; realised variation; outliers.

*Christensen is with CREATES, University of Aarhus, Denmark. E-mail: kchristensen@creates.au.dk. Oomen is with Deutsche Bank, London, UK and affiliated with the Department of Quantitative Economics, the University of Amsterdam, The Netherlands. E-mail: roel.ca.oomen@gmail.com. Podolskij is with the Institute of Applied Mathematics, University of Heidelberg, Germany and affiliated with CREATES, University of Aarhus, Denmark. E-mail: m.podolskij@uni-heidelberg.de. We would like to thank David Bates, Andrew Patton, Kevin Sheppard, Valeri Voev and the participants at the 4th CSDA International Conference on Computational and Financial Econometrics (London, 2010), the Marie Curie High Frequency Research Training Workshop (Berlin, 2011), Queen Mary, University of London, and the Erasmus University, Rotterdam for helpful comments and suggestions. Christensen and Podolskij also gratefully acknowledges financial support from CREATES, which is funded by the Danish National Research Foundation.

1 Introduction

There is a deep consensus in the literature on asset pricing that a realistic dynamic model should incorporate several, if not all, of the following stylised facts: random walk behavior (e.g. Fama, 1965) at a macroscopic level, market microstructure effects (e.g. Niederhoffer and Osborne, 1966) at a microscopic level, as well as stochastic volatility (e.g. Mandelbrot, 1963), leverage (e.g. Black, 1976), and jumps (e.g. Press, 1967). Extensive support for all these factors can be found in both the theory of finance as well as the abundantly available data on all aspects of financial markets. In this paper we bring to bear new econometric techniques on a comprehensive set of tick-by-tick equity and foreign exchange data and are able to penetrate through the microstructure noise to uncover that the jump component appears substantially smaller than what is currently thought. In particular, we provide evidence that the jump component accounts for about 1% of total asset price variability (i.e. quadratic variation) in sharp contrast to the consensus in the literature which is an order of magnitude larger. Our microscopic look at the tick-by-tick data provides the intuition for this result: a burst of volatility is often spuriously identified as a jump at the lower frequencies commonly used in the literature. Of course, there is no doubt that in times of stress, asset prices do move sharply over short periods of time, and while occasionally genuine price jumps do occur, more often than not we find that price continuity is preserved even when accompanied with severe deterioration of liquidity.

The foundations of most asset pricing models can be cast in the class of arbitrage-free Itô semimartingales. These processes are naturally decomposed into a continuous diffusive Brownian component and a discontinuous jump part. The importance of being able to separate out and distinguish between these two fundamentally different sources of risk is emphasized in Aït-Sahalia (2004). Specifically, jumps have profoundly distinct impact on option pricing (e.g. Cox and Ross, 1976; Merton, 1976; Duffie, Pan, and Singleton, 2000), risk management (e.g. Duffie and Pan, 2001; Bakshi and Panayotov, 2010), and asset allocation (e.g. Jarrow and Rosenfeld, 1984; Liu, Longstaff, and Pan, 2003). Empirical work on identifying and modeling the jump component now spans nearly half a century. Table 1 attempts to provide a representative but necessarily incomplete overview. Starting with the influential paper of Press (1967), and up to Jorion (1988), a number of papers estimate a (constant volatility) jump-diffusion model and report very substantial levels of jump variation (JV hereafter, defined as the jump variation expressed as a fraction of total return variation) in excess of 20%. An important shortcoming of the Press (1967)- or Merton (1976)-style jump-diffusion model is that the jump component is the only mechanism that can account for fat tails of the empirical return distribution so that - in the presence of stochastic volatility - the JV measurements are potentially inflated. From the nineties onwards, a large body of work considers numerous generalizations of the jump-diffusion model that include one or several stochastic volatility components as well as state-dependent jump components. Estimation methods for such models are often highly complex and numerically

Table 1: Selection of literature reporting estimates of the jump variation component.

article	data	period	frequency	model	jump variation
Press (1967)	10 DJIA constituents	1926 – 1960	monthly	JD	$20\%^{a}$
Beckers (1981)	47 US large-cap stocks	1975 – 1977	daily	JD	$25\%^{b}$
Ball and Torous (1983)	47 US large-cap stocks	1975 – 1977	daily	JD	$50\%^{c}$
Ball and Torous (1985)	30 US large-cap stocks	1981 – 1982	daily	JD	$47\%^{d}$
Jorion (1988)	DM/$ spot	1974 – 1985	weekly	JD	96%
	CRSP index	1974 – 1985	weekly	JD	36%
Bates (1996)	DM/$ options	1984 – 1991	weekly	SVJ	20%
Bakshi, Cao, and Chen (1997)	S&P500 options	1988 – 1991	daily	SVJ	18.9%
Bates (2000)	S&P500 options	1988 – 1993	weekly	SVJ	$30.3\% - 38.5\%$
Andersen, Benzoni, and Lund (2002)	S&P500 spot	1953 – 1996	daily	SVJ	5.5%
Bollerslev and Zhou (2002)	DM/$	1986 – 1996	5 mins	SVJ	7.4%
Pan (2002)	S&P500 spot and options	1989 – 1996	weekly	SVJ	55.7%
Chernov, Gallant et al. (2003)	DJIA spot	1953 – 1999	daily	SVJ	9.4%
Eraker, Johannes, and Polson (2003)	S&P500 spot	1980 – 1999	daily	SVJ	$8.2\% - 14.7\%$
	NASDAQ100 spot	1985 – 1999	daily	SVJ	$6.0\% - 17.0\%$
Eraker (2004)	S&P500 spot and options	1987 – 1990	daily	SVJ	17.1%
Johannes (2004)	US Treasury bills	1965 – 1999	daily	SVJ	50%
Maheu and McCurdy (2004)	11 US large-cap stocks	1962 – 2001	daily	GARCH	$29\%^{e}$
	DJIA spot	1960 – 2001	daily	GARCH	16.6%
	NASDAQ100 spot	1985 – 2001	daily	GARCH	14.4%
	TXX spot	1995 – 2001	daily	GARCH	22.8%
Barndorff-Nielsen and Shephard (2004)	DM/$	1986 – 1996	5 mins	RV	3.1%
Huang and Tauchen (2005)	S&P500 futures	1982 – 2002	5 mins	RV	4.4%
	S&P500 spot	1997 – 2002	5 mins	RV	7.3%
Barndorff-Nielsen and Shephard (2006)	DM/$, USDJPY	1986 – 1996	$5 - 120$ mins	RV	$5.0\% - 21.9\%$
Bates (2006)	S&P500 spot	1953 – 1996	daily	SVJ	12.7%
Andersen, Bollerslev, and Diebold (2007)	DM/$	1986 – 1999	5 mins	RV	7.2%
	S&P500 spot	1990 – 2002	5 mins	RV	14.4%
	US Treasury bonds	1990 – 2002	5 mins	RV	12.6%
Bollerslev, Law, and Tauchen (2008)	40 US large-cap stocks	2001 – 2005	17.5 mins	RV	12%
	equally weighted index	2001 – 2005	17.5 mins	RV	9%
Jiang and Oomen (2007)	S&P500 spot	1987 – 1995	5 mins	SVJ	$18.6\% - 19.5\%$
Aït-Sahalia and Jacod (2009b)	INTC & MSFT	2006	$5 - 120$ secs	RV	$25\%^{f}$
Bollerslev, Kretschmer et al. (2009)	S&P500 futures	1985 – 2004	5 mins	RV	6.8%
Corsi and Renò (2009)	S&P500 futures	1990 – 2007	5 mins	RV	$6\%^{g}$
Todorov (2009)	S&P500 futures	1990 – 2002	5 mins	RV	15%
Bates (2011)	CRSP index, S&P500	1926 – 2006	daily	SVJ	$6.4\% - 7.2\%$
Patton and Sheppard (2011)	S&P500 ETF	1997 – 2008	5 mins^{h}	RV	15%
Tauchen and Zhou (2011)	S&P500 spot	1986 – 2005	5 mins	RV	5.4%
	US Treasury bonds	1991 – 2005	5 mins	RV	19.1%
	USDJPY	1997 – 2004	5 mins	RV	6.5%
Andersen, Bollerslev, and Huang (2011)	S&P500 futures	1990 – 2005	5 mins	RV	4.9%
	US Treasury bonds	1990 – 2005	5 mins	RV	14.6%

Note. "JD", "SVJ", and "GARCH" refer to the Press (1967), Merton (1976)-type jump-diffusion model, the class of stochastic volatility plus jump models, and GARCH-type models respectively. "RV" refers to the class of model-free measures of variation, including realised variance and power variation.
a. individual JV between $0\% - 100\%$; *b.* individual JV between $10\% - 55\%$; *c.* individual JV between $10\% - 80\%$; *d.* individual JV between $8\% - 93\%$; *e.* individual JV between $20\% - 41\%$. Two stocks have shorter sample from 1980s - 2001; *f.* Includes an infinite activity jump component; *g.* smoothed JV between $2\% - 20\%$; *h.* 5 minute sampling frequency equivalent in trade time

Figure 1: S&P flash-crash episode: Jump or burst in volatility?

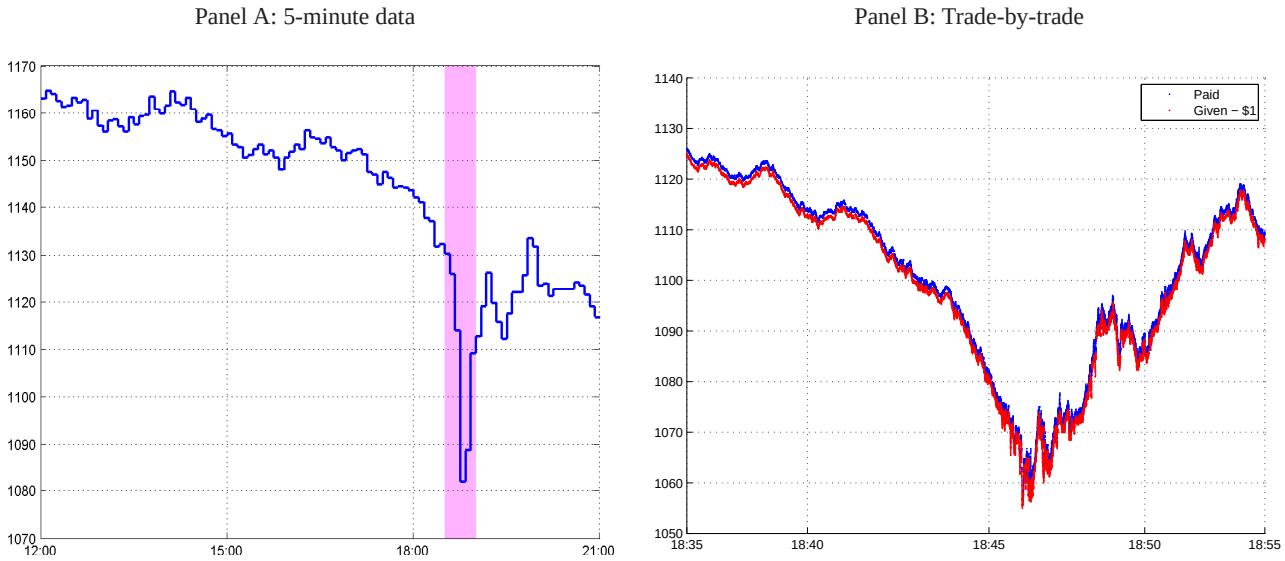

Note. We plot data for the Chicago Mercantile Exchange (CME) E-mini S&P500 futures on May 6, 2010 with time reported in GMT. In Panel B, "Paid" and "given" denote aggressive buy- and sell-orders, respectively. The "given" data has been offset by $1 in order to improve the visual layout.

intensive (e.g. Eraker, Johannes, and Polson, 2003). Also, they can exploit the information in the spot price (e.g. Andersen, Benzoni, and Lund, 2002), its associated derivative prices (e.g. Bates, 1996), or both (e.g. Pan, 2002). The majority of this literature concentrates on the US large-cap S&P500 equity index and typically finds that the JV is around $10\% - 20\%$. The corresponding figure for foreign exchange rates is comparable and that of Treasury bills and individual stocks still higher. The most recent work on jumps has seen a shift away from model-based inference on low-frequency data to model-free inference based on intra-day data. In an influential series of papers, Barndorff-Nielsen and Shephard (2004, 2006); Barndorff-Nielsen, Shephard, and Winkel (2006) introduce the concept of (bi-) power variation – a simple but very effective technology to identify and measure the variation of jumps from intra-day data (see Aït-Sahalia and Jacod, 2009b,c; Mancini, 2004, 2009, for a related jump-robust threshold estimator). Using this, or variations thereof, a large number of recent articles now report model-free JV estimates (e.g. Huang and Tauchen, 2005; Andersen, Bollerslev, and Diebold, 2007) that are around 10% for the S&P500 index and thus reinforce the earlier literature that the jump component is important.

Jumps are defined as *instantaneous* and *discrete* moves in the price, and it is therefore quite intuitive that identification is helped by having available the finest resolution price view possible. Indeed, this is precisely what motivates the recent literature to use intra-day data. However, the consensus 5-minute frequency at which returns are typically sampled – rather than at the finer tick-by-tick resolution – reflects a compromise where market microstructure effects are sufficiently

benign for the theory to remain valid. Figure 1 illustrates the cost of doing so: a diminished ability to distinguish jumps from bursts in volatility. From Panel A, where returns are sampled at a 5-minute frequency, we would likely conclude that the notorious "flash-crash" episode (see e.g. Easley, de Prado, and O'Hara, 2011, for a discussion of the event) contains a number of very large "jumps". Indeed, the bipower variation jump measure is highly significant indicating the presence of jumps on formal statistical grounds. Yet, when zooming in on the relevant sub-period, from Panel B we see that at trade-by-trade frequency jumps are elusive. In fact, in a recent study using audit trail data Kirilenko, Kyle, Samadi, and Tuzun (2011) characterize the flash-crash as a "brief period of extreme market volatility". The March 11, 2011 earthquake in Japan led to similar episodes in the USDJPY currency rate which experienced a flash-crash type episode on March 16 over an intense sell-off[1] and on March 18 over a coordinated intervention by Bank of Japan and other G7 central banks. Again, as is clear from Figure 8 later in the paper, both events would be classified as exhibiting large jumps by conventional realised measures based on 5-minute data, while the tick data reveal a period of heightened volatility rather than discrete price jumps.

The contribution this paper makes is to provide a detailed and comprehensive study into the magnitude of the jump component based on the highest data resolution available. To the best of our knowledge, this paper is the first to do so and, as already mentioned above, we find that the tick data have a very different story to tell. Our analysis employs the new pre-averaging techniques of Podolskij and Vetter (2009a), Jacod, Li, Mykland, Podolskij, and Vetter (2009) to construct noise-robust jump measures, which allow us to exploit the information contained in milli-second time-stamped tick data. We apply these to a representative dataset comprising of US large-cap stocks (i.e. the 30 DJIA constituents), equity indices (i.e. the S&P500 and NASDAQ100), and foreign currency rates (i.e. the EURUSD, USDJPY and USDCHF). We confirm that when sampling at a 5-minute frequency the jump component does appear very substantial – around 10% in line with the extant literature – but as we turn on the microscope and venture into tick space most jumps vanish and we are left with highly volatile episodes instead. The overall jump variation measured across all instruments we consider is just over 1%. This finding of a much diminished magnitude of jumps clearly carries important implications for various finance applications as already highlighted above: for instance, an options trader that follows the market on an hourly basis for the purpose of hedging can *experience* jumps in the price, while an automated hedging algorithm operating in tick-time may not. As we illustrate in the paper, these two scenarios will lead to profoundly different pay-off patterns.

In addition to the above, the paper makes some further methodological contributions. Firstly, to conduct statistical tests on the jump component, a jump-robust and positive semi-definite estimate of the asymptotic covariance matrix

[1]The sell-off is thought to be the result of a combination of factors, including (i) repatriation of funds (or anticipation thereof) to honor insurance claims and to fund reconstruction efforts, (ii) portfolio rebalancing of currency hedged foreign investors after Nikkei fall, (iii) JPY carry traders forced to cut positions on margin calls, (iv) retail stop-loss levels are hit.

is required. We develop and implement a novel estimator that does exactly this. Secondly, we discuss the distinction between price-jumps and price-outliers and show how the triplet of realised variance, bipower variation, and quantile-based realised variance (Christensen, Oomen, and Podolskij, 2010) can be used to disentangle the diffusive, jump, and outlier variation components. To the best of our knowledge, this paper is the first to formally discuss this issue[2] and we provide a consistency result as well as a central limit theorem.

2 Theoretical framework

We study the evolution of the logarithmic price of a financial asset, say $X = (X_t)_{t\geq 0}$, which is defined on a filtered probability space $\left(\Omega, \mathcal{F}, (\mathcal{F}_t)_{t\geq 0}, \mathbb{P}\right)$ and adapted to the filtration $\mathcal{F}_t$ that represents the information available to market participants at time t, $t \geq 0$. To begin with, we assume that X operates in an arbitrage-free frictionless market, which implies that X belongs to the class of semimartingale processes (e.g. Back, 1991; Delbaen and Schachermayer, 1994). As standard in the asset pricing literature, we further assume that X can be represented by a jump-diffusion model, which takes the form

$$X_t = X_0 + \int_0^t a_s \mathrm{d}s + \int_0^t \sigma_s \mathrm{d}W_s + \sum_{i=1}^{N_t^J} J_i, \qquad t \geq 0, \tag{1}$$

where X_t is the log-price at time t, $a = (a_t)_{t\geq 0}$ is a locally bounded and predictable drift term, $\sigma = (\sigma_t)_{t\geq 0}$ is an adapted càdlàg volatility process, $W = (W_t)_{t\geq 0}$ is a standard Brownian motion, $N^J = \left(N_t^J\right)_{t\geq 0}$ is a counting process and $J = (J_i)_{i=1,\ldots,N_t^J}$ is a sequence of non-zero random variables. Here, N^J represents the total number of jumps in X that has occurred up to time t and J are the corresponding jump sizes.

The total quadratic variation of the cumulative return process is then given by

$$[X]_t = \int_0^t \sigma_s^2 \mathrm{d}s + \sum_{i=1}^{N_t^J} J_i^2, \tag{2}$$

i.e. the integrated diffusive variation plus the sum of squared jumps. As such, the quadratic variation is composed of two distinct sources of risk, and it is their relative importance that we are interested in measuring. Specifically, the object of econometric interest is the jump variation defined on the unit interval as:

$$JV = \frac{[X] - \int \sigma_s^2 \mathrm{d}s}{[X]} \tag{3}$$

It should be pointed out that quadratic variation has very close ties with the, perhaps, more familiar concept of conditional variance, which plays a key role in financial economics (e.g. Andersen, Bollerslev, Diebold, and Labys, 2003). We also

[2] Christensen, Oomen, and Podolskij (2010) show robustness of their quantile-based realised variance measure with respect to outliers. Aït-Sahalia and Jacod (2009a) also highlight the relevance of "bounce-backs" in the context of data filtering.

note that $[X]_t$ can equivalently be defined as follows

$$[X]_t = \underset{N\to\infty}{\text{p-lim}} \sum_{i=1}^{N} \left(X_{t_i} - X_{t_{i-1}}\right)^2, \tag{4}$$

for any sequence of partitions $0 = t_0 < t_1 < ... < t_N = t$ with $\sup_i \{t_i - t_{i-1}\} \to 0$ as $N \to \infty$ (e.g. Protter, 2004). It is this fundamental result from stochastic calculus that has motivated the increasing use of high-frequency data to estimate financial volatility.

To prove our central limit theorems (CLTs) below, we impose some structure on σ.

Assumption (V) *σ does not vanish (V_1) and it satisfies the equation:*

$$\sigma_t = \sigma_0 + \int_0^t a'_s \mathrm{d}s + \int_0^t \sigma'_s \mathrm{d}W_s + \int_0^t v'_s \mathrm{d}B'_s, \quad t \geq 0, \tag{V$_2$}$$

where $a' = (a'_t)_{t\geq 0}$, $\sigma' = (\sigma'_t)_{t\geq 0}$ and $v' = (v'_t)_{t\geq 0}$ are adapted càdlàg, $B' = (B'_t)_{t\geq 0}$ is a Brownian motion, and $W \perp\!\!\!\perp B'$ (here $A \perp\!\!\!\perp B$ means that A and B are stochastically independent).[3]

2.1 Realised variation and market microstructure noise

We base our analysis on the theory of realised variation, where tick-by-tick data are used to make inference about the latent diffusive volatility and jumps.[4] More specifically, we assume that an equidistant high-frequency record of X is available at time points $t_i = i/N$, for $i = 0, 1, \ldots, N$. Here and throughout the remainder of the paper, we normalize the time window to the unit interval $[0, 1]$ for ease of exposition. We construct N continuously compounded returns as

$$\Delta_i^N X = X_{i/N} - X_{(i-1)/N}, \quad \text{for } i = 1, \ldots N. \tag{5}$$

Then, an estimator of $[X]_1$ is given by the realised variance (RV hereafter)

$$RV_N[X] = \sum_{i=1}^{N} |\Delta_i^N X|^2. \tag{6}$$

[3]Assumption (V) amounts to saying that σ is of continuous semimartingale form. We should note the appearance of W in σ, which allows for leverage effects (e.g. Christie, 1982). If X itself is a continuous process, then the assumption is a weak regularity condition, which is fulfilled for many financial models. Let X be a unique, strong solution of a stochastic differential equation. Then, for example, under some smoothness conditions on the volatility function $\sigma = \sigma(t, X_t)$, assumption (V$_2$) (with $v'_s = 0$ for all s) is a direct consequence of Itô's Lemma. If X is not continuous, as in Eq. (1), then σ is potentially discontinuous as well. In fact, there is some empirical support for allowing σ to jump, e.g. Eraker, Johannes, and Polson (2003). We could include that case here at the cost of substantial extra technical rigor. Thus, even though assumption (V) is not a necessary condition, it simplifies some of our proofs considerably. A more general treatment in the high-frequency setting, including the case where σ jumps, is covered in Barndorff-Nielsen, Graversen, Jacod, Podolskij, and Shephard (2006). We rule out these technical details here, as they are not important to our exposition.

[4]Comprehensive reviews of this literature can be found in Andersen, Bollerslev, and Diebold (2010); Barndorff-Nielsen and Shephard (2007).

Consistency follows as a direct consequence of Eq. (4), i.e. $RV_N[X] \xrightarrow{p} [X]_1$ as $N \to \infty$.

A popular way to separate out the diffusive- and jump-variation components from $[X]_1$ is via the use of a jump-robust estimator of the integrated variance. To this end, Barndorff-Nielsen and Shephard (2004) introduce bipower variation (BV hereafter)[5]:

$$BV_N[X] = \frac{N}{N-1}\frac{1}{\mu^2}\sum_{i=2}^{N}|\Delta_{i-1}^N X||\Delta_i^N X|, \tag{7}$$

where $\mu = E[|N(0,1)|] = \sqrt{2/\pi}$ and the factor $N/(N-1)$ is a small sample correction. Because $BV_N[X] \xrightarrow{p} \int_0^1 \sigma_s^2 \mathrm{d}s$ as $N \to \infty$, the jump variation component – in the noiseless case – can be estimated consistently as:

$$RV_N[X] - BV_N[X] \xrightarrow{p} \sum_{i=1}^{N_1^J} J_i^2. \tag{8}$$

It is long-established that the trading process pollutes the underlying efficient price with measurement error that is a result of market imperfections such as bid-ask spreads and price discreteness (e.g. Niederhoffer and Osborne, 1966; Roll, 1984; Black, 1986). This microstructure noise has been shown to have a detrimental impact on the standard realised measures of return variation (such as RV and BV above) and renders them biased and inconsistent when computed using noisy data (see, e.g., Zhou, 1996; Hansen and Lunde, 2006). Below, we explicitly account for the presence of microstructure noise by assuming that the observed price process Y is related to the underlying price process X as:

$$Y = X + u. \tag{9}$$

where u is an i.i.d. noise process with $E(u) = 0$ and $E(u^2) = \omega^2$, and u is independent of X, or $u \perp\!\!\!\perp X$.[6] Thus, the challenge we need to address is to how infer the diffusive- and jump-variation components from discretely sampled and noisy observations of the underlying price process.

[5] Alternative ways of estimating the integrated variance in the presence of jumps exist. Aït-Sahalia and Jacod (2009b,c); Mancini (2004, 2009), for example, propose to robustify the RV directly via threshold elimination of "large" returns, while Andersen, Dobrev, and Schaumburg (2008); Christensen, Oomen, and Podolskij (2010) suggest to infer diffusive volatility from the quantiles of high-frequency returns. We shall draw upon both these strands of the literature below. Recent developments also show how to improve the finite sample jump robustness of the BV or make it more efficient, see Corsi, Pirino, and Renò (2010); Mykland, Shephard, and Sheppard (2010).

[6] The i.i.d, independent of X, noise assumption is analytically convenient and also has some empirical support at moderate sampling frequencies (e.g. Hansen and Lunde, 2006; Diebold and Strasser, 2008), but it is not binding. The interested reader can consult Jacod, Li, Mykland, Podolskij, and Vetter (2009), where a more general treatment of the noise is given. Our results extend along those lines as well.

2.2 Noise-robust jump estimation

To make inference about $[X]_1$ and its components using observations of Y, we make use of the pre-averaging approach introduced by Jacod, Li, Mykland, Podolskij, and Vetter (2009); Podolskij and Vetter (2009a,b).[7] Intuitively, the pre-averaging method locally smooths the observed asset price Y so that the microstructure component u (almost) disappears under averaging. The resulting pre-averaged returns can then be used to construct consistent measures of the diffusive- and jump-variation components as we outline below.

First, we choose a pre-averaging horizon; a sequence of integers $K = K(N)$, which satisfies

$$K = \theta\sqrt{N} + o(N^{-1/2}). \tag{10}$$

Throughout the paper, we use $K = \lceil \theta\sqrt{N} \rceil$. Second, we choose a real-valued weight function used to conduct the averaging $g : [0,1] \to \mathbb{R}$.[8]

We are also going to use the following constants that are associated with g:

$$\psi_1 = \int_0^1 \left(g'(s)\right)^2 \mathrm{d}s, \qquad \psi_2 = \int_0^1 g^2(s)\,\mathrm{d}s. \tag{11}$$

Remark 1 In practice, we use the Riemann approximations

$$\psi_1^K = K\sum_{j=1}^{K}\left[g\left(\frac{j}{K}\right) - g\left(\frac{j-1}{K}\right)\right]^2, \qquad \psi_2^K = \frac{1}{K}\sum_{j=1}^{K-1} g^2\left(\frac{j}{K}\right) \tag{12}$$

of ψ_1 and ψ_2 to improve finite sample accuracy.

With this equipment in place, we can pre-average noisy returns

$$\bar{Y}_i^N = \sum_{j=1}^{K-1} g\left(\frac{j}{K}\right)\Delta_{i+j}^N Y, \quad \text{for } i = 0,\ldots,N-K+1. \tag{13}$$

In what follows, we use the weight function $g(x) = \min(x, 1-x)$. This is a natural candidate in our setting, because with this choice of g and if K is even, it holds that

$$\bar{Y}_i^N = \frac{1}{K}\sum_{j=K/2}^{K-1} Y_{\frac{i+j}{N}} - \frac{1}{K}\sum_{j=0}^{K/2-1} Y_{\frac{i+j}{N}}, \tag{14}$$

[7] When the object to be estimated is quadratic variation, the pre-averaging approach is to first-order equivalent to the realised kernel-based estimator of Barndorff-Nielsen, Hansen, Lunde, and Shephard (2008) and the two-scale or multi-scale subsampler of Zhang, Mykland, and Aït-Sahalia (2005) and Zhang (2006).

[8] At a technical level, g has to be continuous, piecewise continuously differentiable such that its derivative g' is piecewise Lipschitz. Moreover, we require $g(0) = g(1) = 0$ and $\int_0^1 g^2(u)\mathrm{d}u > 0$.

which makes the use of the term "pre-averaging" transparent.

We should point out that while pre-averaging smooths out noise, it does not impair our ability to identify the jump component. The intuition for this is that, although pre-averaging does enforce some continuity on the price path, it also smooths out the diffusive return variation by an equivalent factor, thereby keeping the relative contribution of stochastic volatility and jumps intact. We further demonstrate this with the convergence results in Proposition 1 and with finite sample experiments in the simulation section.

Next, we can introduce noise-robust versions of the RV and BV:

$$RV_N^*[Y] = \frac{N}{N-K+2}\frac{1}{K\psi_2^K}\sum_{i=0}^{N-K+1}|\bar{Y}_i^N|^2 - \frac{\psi_1^K}{\theta^2\psi_2^K}\omega^2, \tag{15}$$

$$BV_N^*[Y] = \frac{N}{N-2K+2}\frac{1}{K\psi_2^K\mu_1^2}\sum_{i=0}^{N-2K+1}|\bar{Y}_i^N||\bar{Y}_{i+K}^N| - \frac{\psi_1^K}{\theta^2\psi_2^K}\omega^2. \tag{16}$$

The terms $N/(N-K+2)$ and $N/(N-2K+2)$ are small sample corrections, which adjust for the actual number of summands involved in the computations. The factor $\frac{\psi_1^K}{\theta^2\psi_2^K}\omega^2$ is a bias-correction removing a leftover effect of the noise, which is needed because pre-averaging does not completely wipe out the influence of the noise. The bias depends on the unknown noise variance ω^2, which can be estimated using a variety of available estimators, e.g. the sum-of-squares estimator proposed by Bandi and Russell (2006): $\hat{\omega}^2_{\text{RV}} = \frac{1}{2N}\sum_{i=1}^N|\Delta_i^N Y|^2$; the autocovariance estimator: $\hat{\omega}^2_{\text{AC}} = -\frac{1}{N-1}\sum_{i=2}^N \Delta_{i-1}^N Y \Delta_i^N Y$ as in Oomen (2006) or a parametric maximum likelihood estimator of Aït-Sahalia, Mykland, and Zhang (2005), see Gatheral and Oomen (2010) for a comparison of these and other estimators. In the simulations and empirical application below, we use $\hat{\omega}^2_{\text{AC}}$, while noting that our results are largely unaffected by the specific choice of noise variance estimator (in part, because the bias correction term drops out when constructing the difference $RV_N^*[Y] - BV_N^*[Y]$).

2.3 Consistency and asymptotic distribution

The next proposition, which is adapted directly from previous work by Podolskij and Vetter (2009a), states the probability limit of the pre-averaging estimators in the pure noise model, and their joint asymptotic distribution under the null hypothesis of no jumps. A robustness analysis given below further extends the proposition by showing that it remains true in a generalisation of the model in Eq. (9), which incorporates the presence of finite-activity outlier processes.

Proposition 1 *Assume that Y follows Eq.* (9) *and that $E(u^4) < \infty$. As $N \to \infty$, it holds that*

$$RV_N^*[Y] \xrightarrow{p} [X]_1, \qquad BV_N^*[Y] \xrightarrow{p} \int_0^1 \sigma_s^2 \mathrm{d}s. \tag{17}$$

Moreover, suppose in addition that X is a continuous semimartingale, i.e. X follows Eq. (1) *but with $N_t^J \equiv 0$ for all t, and with condition (V) fulfilled. Finally, assume that $E(u^8) < \infty$. As $N \to \infty$, it then further holds that*

$$N^{1/4} \begin{pmatrix} RV_N^*[Y] - \int_0^1 \sigma_s^2 \mathrm{d}s \\ BV_N^*[Y] - \int_0^1 \sigma_s^2 \mathrm{d}s \end{pmatrix} \xrightarrow{d_s} MN(0, \Sigma^*), \tag{18}$$

a mixed normal distribution with conditional covariance matrix Σ^*, where Σ^* is defined in Appendix B.[9]

Proof See Podolskij and Vetter (2009a).

The consistency result of Theorem 1 unveils that, in the presence of noise, we can measure jumps by taking

$$RV_N^*[Y] - BV_N^*[Y] \xrightarrow{p} \sum_{i=1}^{N_1^J} J_i^2. \tag{19}$$

The CLT then supplies the basis for a nonparametric noise-robust jump test. We should point out that the $N^{-1/4}$ rate of convergence, which is slow compared to the noiseless case, is still the fastest possible that can be achieved in noisy diffusion models (Gloter and Jacod, 2001a,b).

Taking differences between $RV_N^*[Y]$ and $BV_N^*[Y]$, and using the properties of stable convergence, we can apply the delta method to the distribution theory in Proposition 1 to deduce that under the null of no jumps

$$\frac{N^{1/4}(RV_N^*[Y] - BV_N^*[Y])}{\sqrt{\Sigma_{11}^* + \Sigma_{22}^* - 2\Sigma_{12}^*}} \xrightarrow{d} N(0,1), \tag{20}$$

where $(\Sigma_{ij}^*)_{1 \le i,j \le 2}$ denote the individual entries of Σ^*. Under the alternative hypothesis, the convergence $RV_N^*[Y] - BV_N^*[Y] \xrightarrow{p} \sum_{i=1}^{N_1^J} J_i^2$ follows from Eq. (19), which means that conditional on the presence of jumps, the test is consistent as $N \to \infty$.

2.4 Estimating Σ^*

As usual, the CLT in Proposition 1 is an infeasible result, because the matrix Σ^*, which holds the covariance structure of the bivariate vector $(RV_N^*[Y], BV_N^*[Y])$, is not known in practice. In order to construct a feasible noise-robust jump test that can be implemented on actual data, we therefore need to estimate Σ^*.

[9] Throughout the paper, the symbol "$\xrightarrow{d_s}$" is used to denote convergence in law stably. We refer to Barndorff-Nielsen, Hansen, Lunde, and Shephard (2008) for a formal definition of stable convergence in law and the motivation for using this type of convergence in the high-frequency volatility setting.

Figure 2: Illustration of block subsampler.

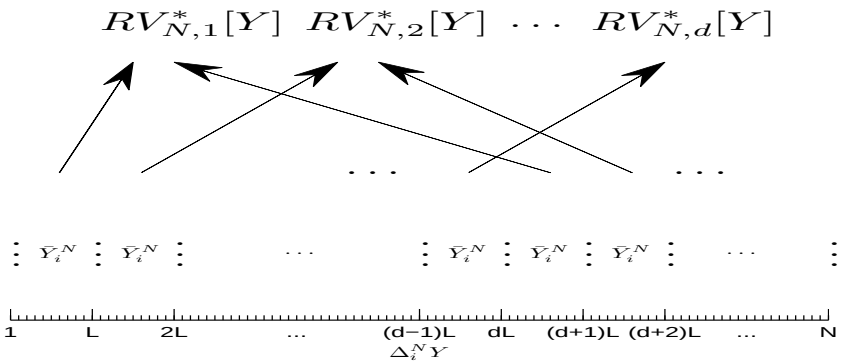

Note. This figure illustrates the construction of the subsampled $RV^*_{N,m}[Y]$ estimators, which are used as input to compute the block subsample estimator of the covariance matrix Σ^*.

Podolskij and Vetter (2009a) propose consistent estimators of the elements of Σ^*, $(\Sigma^*_{ij})_{1\leq i,j\leq 2}$. We could adopt this approach as well by designing consistent estimators of the individual entries of Σ^*, for example using

$$\hat{\Sigma}^*_{11} = \frac{N^{-1/2}}{\theta^2\psi_2^2}\sum_{i=K}^{N-2K+1}|\bar{Y}_i^N|^2\left(\sum_{l=-K+1}^{K-1}\left(|\bar{Y}_{i+l}^N|^2 - |\bar{Y}_{i+K}^N|^2\right)\right) \xrightarrow{p} \Sigma^*_{11}. \tag{21}$$

The problem with this way of getting at Σ^* is that once we put the pieces back together, the estimate of the full covariance matrix $\hat{\Sigma}^*$ is not guaranteed to be positive semi-definite.

Instead, we propose a novel block subsample estimator of Σ^*, which has a very intuitive form and is positive semi-definite by definition.[10]. To describe the construction of this estimator, we first choose two frequencies d and L, such that $L >> K$, $dL = o(N)$ and $L, d \to \infty$ as $N \to \infty$. Here, d is the number of subsamples and L is a block length.

Second, we let

$$RV^*_{N,m}[Y] = \frac{d}{K\psi_2^K}\sum_{i\in J_m}|\bar{Y}_i^N|^2 - \frac{\psi_1^K}{\theta^2\psi_2^K}\hat{\omega}^2_{\text{AC}}, \tag{22}$$

for $m = 1, \ldots, d$, where $J_m = \{i : 0 \leq i \leq N-K+1 \text{ and } (m-1+jd)L \leq i < (m+jd)L-K+1 \text{ for some } j \in \mathbb{N}\}$. As such, $RV^*_{N,m}[Y]$ is a subsampled version of the pre-averaged RV defined above.

The construction of $RV^*_{N,m}[Y]$ is depicted in Figure 2, which shows how we block, allocate and pre-average the noisy return series $(\Delta_i^N Y)$ to assemble the various subsample estimates. Note that pre-averaging is done locally within each block of length L, and that there is no pre-averaging carried out between blocks. As a consequence, the sequence

[10]This relates to recent work by Kalnina (2011).

$RV^*_{N,m}[Y]$, $m = 1, \ldots, d$, all fulfill the CLT of $RV^*_N[Y]$ from Proposition 1, except with a slower rate of convergence $N^{1/4}/d^{1/2}$. It also follows that the $RV^*_{N,m}[Y]$ estimates are mutually independent, asymptotically, because they are computed from non-intersecting increments.

Hence, it is intuitive that

$$\hat{\Sigma}^*_{11} = \frac{1}{d}\sum_{m=1}^{d}\left(\frac{N^{1/4}}{d^{1/2}}\left(RV^*_{N,m}[Y] - \int_0^1 \sigma_s^2 \mathrm{d}s\right)\right)^2 \tag{23}$$

is a good proxy for Σ^*_{11}. But the integrated variance is latent, so we replace it by $RV^*_N[Y]$ – the original pre-averaged RV. Now, we can construct the sequence $BV^*_{N,m}[Y]$ using the exact same principles. Then, we define

$$T^*_{N,m}[Y] = \frac{N^{1/4}}{d^{1/2}}\left(RV^*_{N,m}[Y] - RV^*_N[Y], BV^*_{N,m}[Y] - BV^*_N[Y]\right)', \tag{24}$$

and compute

$$\hat{\Sigma}^* = \frac{1}{d-1}\sum_{m=1}^{d} T^*_{N,m}[Y]T^*_{N,m}[Y]'. \tag{25}$$

Proposition 2 *Assume that Y follows Eq.* (9)*, where X follows the jump-diffusion model in Eq.* (1) *and $E(u^4) < \infty$. Moreover, we assume that $\sqrt{N}/d^2 \to 0$. As $N \to \infty$, it then holds that*

$$\hat{\Sigma}^* \xrightarrow{p} \Sigma^*. \tag{26}$$

Proof See appendix.

We can then execute the feasible jump test by plugging the estimates in Eq. (25) into Eq. (20).

A couple of further remarks are in place here. First, the finite sample corrections that help to improve small sample accuracy of $RV^*_N[Y]$ and $BV^*_N[Y]$ are also applied to $BV^*_{N,m}[Y]$ and $RV^*_{N,m}[Y]$. Second, as the unobserved integrated variance is replaced by an estimator, we find better finite sample accuracy by correcting the covariance matrix estimator for a "loss of degree of freedom", which is why we are dividing by $d-1$ in Eq. (25). Third, the condition $\sqrt{N}/d^2 \to 0$ implies that $d = O(N^\epsilon)$, for some $0.25 < \epsilon < 0.50$, which ensures that $\hat{\Sigma}^*$ is consistent for Σ^* both under the null and alternative hypothesis, as shown in the proof of Proposition 2. This point is important, because it means that in principle we do not need to worry about eroding the power of the jump test (Barndorff-Nielsen and Shephard, 2006). Still, the estimator appears sensitive to jumps in finite samples, and we propose one further adjustment of $\hat{\Sigma}^*$ in the simulation section below. Fourth, while the choice of d and L affect the efficiency of the estimator, a theory for deriving an optimal choice of these tuning parameters is at best complicated and we leave this analysis for future research. Instead, we choose a simple calibration of $\hat{\Sigma}^*$, which seems to work reasonably well in simulations and practice.

Table 2: Properties of the pre-averaging estimators.

	$RV_N^*[Y]$			$BV_N^*[Y]$			$BV_N^*[Y](\tau)$		
$\theta =$	0.10	0.25	0.50	0.10	0.25	0.50	0.10	0.25	0.50
BM	1.00	1.00	1.00	1.00	1.00	1.00	1.00	1.00	1.00
SV2F	1.00	1.00	1.00	1.00	1.00	1.00	1.00	1.00	1.00
BMJ	1.25	1.25	1.25	1.03	1.04	1.05	1.00	1.00	1.00
BMO	1.00	1.00	1.00	0.99	1.00	1.00	1.01	1.00	1.00

Note. This table reports the mean of the pre-averaging estimators $RV_N^*[Y]$, $BV_N^*[Y]$, and $BV_N^*[Y](\tau)$ (normalised by $\int_0^1 \sigma_s^2 \mathrm{d}s$) over $10,000$ simulation runs where $N = 10,000$, $\gamma = 0.50$.

3 Simulation study

In this section, we perform controlled Monte Carlo experiments to gauge the finite sample accuracy of the noise-robust pre-averaging theory introduced above. In particular, we examine the ability of these estimators to back out the diffusive- and jump-variation components in the presence of microstructure noise. We also inspect the statistical properties of the jump testing framework.

Below, we simulate log-prices X from four distinct models, namely (i) a Brownian motion or "BM" model where $\mathrm{d}X_t = \sigma_t \mathrm{d}W_t$ with $\sigma_t^2 = 0.0391$ corresponding to a return volatility of about 20% annualized, (ii) a two-factor stochastic volatility model with leverage or "SV2F" proposed by Chernov, Gallant, Ghysels, and Tauchen (2003), using calibrated parameter values reported in Huang and Tauchen (2005), (iii) a Brownian motion plus jump or "BMJ" model, where we position a jump of random size at a random point in the series, ensuring that on average it accounts for 20% of total variation, and (iv) a Brownian motion plus outlier or "BMO" model, where we position an outlier of random size at a random point in the series, ensuring that on average it accounts for 20% of total variation. These choices of models allow us to gauge the ability of the pre-averaged estimators to account for stochastic volatility and study their robustness to jumps and outliers (the latter case is discussed in more detail below, see Section 6). Using an Euler discretization scheme, we simulate $10,000$ independent price paths for each model, fixing the sample size at $N = 10,000$. To obtain the noise contaminated observed price path Y, we select ω^2 by fixing the noise ratio (Oomen, 2006) $\gamma = \sqrt{N\omega^2 / \int_0^1 \sigma_s^2 \mathrm{d}s} = 0.50$. As can be seen from Table 3, our choice of γ and N are realistic albeit relatively conservative.

Table 2 reports the mean of the pre-averaging estimators $RV_N^*[Y]$ and $BV_N^*[Y]$ – normalised by the diffusive variation component $\int_0^1 \sigma_s^2 \mathrm{d}s$ – for three choices of the tuning parameter $\theta = \{0.10; 0.25; 0.50\}$ where $K = \lceil \theta\sqrt{N} \rceil$. From the above, we would expect that $E(RV_N^*[Y]) = 1$ for the BM, SV2F, and BMO models, $E(RV_N^*[Y]) = 1.25$ for BMJ,

and $E(BV_N^*[Y]) = 1$ for all models due to its robustness to jumps. The simulated values largely agree with these figures irrespective of the pre-averaging parameter θ. Only for the pre-averaged BV measure in the presence of jumps do we observe a (small) upward bias that grows with θ. If left untreated, this bias translates into a downward bias of the estimated jump proportion and will also reduce the power of the jump test. Motivated by this, we supplement the jump-robust $BV_N^*[Y]$ with a threshold filter, which is discussed in the next subsection. The last column of Table 2 shows that this modified measure largely eliminates the bias and can thus be used to conduct reliable inference about jumps.

3.1 Threshold pre-averaged bipower variation

To reduce the finite sample bias induced by jumps in the ordinary BV defined by Eq. (7), Corsi, Pirino, and Renò (2010) propose to augment the estimator with a threshold filter. The main idea is to first pre-trim the data in order to eliminate large jumps, and then rely on the machinery of the BV to wipe out the small jumps. It appears natural to use such a device for our pre-averaged jump-robust estimator of integrated variance as well. As already mentioned, this should also help to improve the power of the jump test by providing a less downward biased measure of jumps.

Setting a good threshold can be accomplished by noting that under a scaled Brownian motion with i.i.d noise, as in model BM above, the asymptotic distribution (as $N \to \infty$) of $\bar{Y}_i^N$ is given by:

$$N^{1/4}\bar{Y}_i^N \mid \mathcal{F}_{i/N} \overset{a}{\sim} N\left(0, \psi_2\sigma^2\theta + \psi_1\omega^2\frac{1}{\theta}\right). \tag{27}$$

Thus, we can define a threshold by taking

$$\tau = q_\alpha \times \sqrt{\psi_2^K\sigma^2\theta + \psi_1^K\omega^2\frac{1}{\theta}} \times N^{-\varpi},$$

where q_α is the α-quantile from the $N(0,1)$ distribution and $\varpi \in (0, 0.25)$. Of course, in order to set a value of τ in practice, we substitute plug-in estimators for unknown parameters, i.e. σ^2 and ω^2. Moreover, it requires selection of α and ϖ. Throughout, the noise variance is estimated with $\hat{\omega}^2_{\text{AC}}$ and we use $\alpha = 0.999$ and $\varpi = 0.20$, which produces satisfactory results in the simulations across models. σ^2 is proxied with $BV_N^*[Y]$, noting that, as the pre-averaged BV is slightly upward biased in finite samples with jumps in the data, the last step should lead to setting conservative threshold levels, thereby avoiding overtrimming the data.

After τ is set, we could proceed by excluding all terms for which $|\bar{Y}_i^N| > \tau$, when computing the $BV_N^*[Y]$. However, we found this to be suboptimal, as it tends to remove too large fractions of data in finite samples. To understand this feature, it helps to consider Figure 3. In Panel A, we plot the first 100 noisy returns from a replication of the BMJ model, while the corresponding 77 pre-averaged data, using $\theta = 0.25$ for purpose of illustration, are shown in Panel B. The threshold level τ is computed as detailed above. A large jump occurs in the 52nd noisy return, and it creates a hump in

Figure 3: Illustration of threshold filtering procedure.

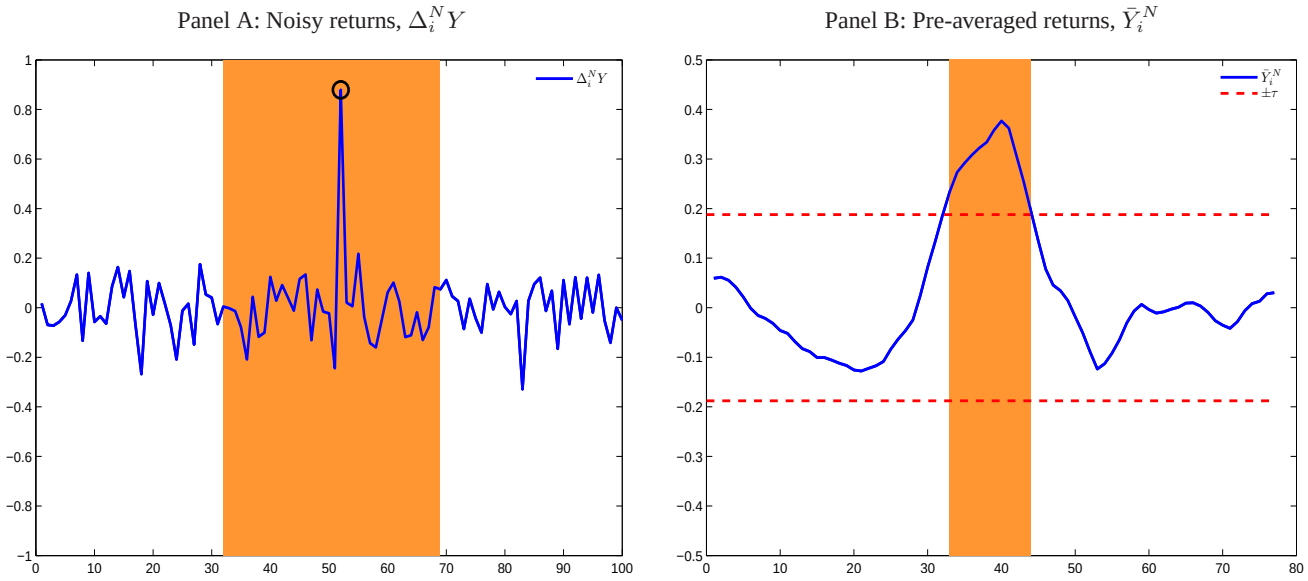

Note. To the left is the noisy return series, $(\Delta_i^N Y)$, while the pre-averaged return series, $(\bar{Y}_i^N)$, is to the right. The threshold τ is the plotted with dashed red lines (- -). The orange area (■) in the left panel shows the part of $(\Delta_i^N Y)$ taken out for inspection, while the black circle (**o**) highlights the return that is selected to be discarded.

the pre-averaged returns, corresponding roughly to the graph of the weight function $g(x) = \min(x, 1-x)$. This induces a long sequence of breaches of τ, and if the naive filter was to be used, this single large jump calls for discarding no less than twelve pre-averaged returns in this example – all those that fall outside the threshold boundaries. Moreover, many of the surrounding observations not crossing τ remain inflated.

Set against this backdrop, we proceed with a matching algorithm that exploits the link between the (ΔY_i^N) and $(\bar{Y}_i^N)$ series. To illustrate the mechanics, we consider Figure 3 again. In Panel B, when a breach of τ is found, we go back and inspect the subset of all noisy returns, which are used to compute that particular sequence of pre-averaged returns, as highlighted in both subpanels. Finally, we select the largest noisy return, in magnitude, to be discarded. In any given simulation, if multiple violations of τ are observed, we repeat this step until all extreme noisy returns have been removed, after which we reconstruct the pre-averaged return series based on the reduced sample.[11]

Table 2 highlights the properties of the truncated version of pre-averaged BV: the estimator continues to deliver unbiased estimates of the integrated variance for the diffusive BM and SV2F models but it now also largely eliminates the finite sample bias in the presence of jumps.

[11] Of course, the trimming step can be iterated on the new set of pre-averaged data, but we found no or little gains from doing this.

3.2 Jump testing

To arrive at a feasible version of the jump test, we implement the block subsampler estimator proposed in Section 2.4 using $d = 20$ subsample estimates and a block length of $L = 5K$. Unreported simulations show that this choice of tuning parameters delivers estimates of Σ^*, which are roughly unbiased. To check if a transformation of Eq. (20) could enhance finite sample approximation of the asymptotic distribution, we also experiment with a log-based and ratio-type t-statistic, as in, e.g., Huang and Tauchen (2005). We found that both transformations improved upon the raw distributional result, while delivering almost identical finite sample accuracy between the two. Hence, to save space we only report the outcome of the log-based distribution theory, relying on the delta method for stable convergence to obtain

$$\frac{N^{1/4}(\ln RV_N^*[Y] - \ln BV_N^*[Y](\tau))}{\sqrt{\Sigma_{11}^* + \Sigma_{22}^* - 2\Sigma_{12}^*}/\int_0^1 \sigma_s^2 \mathrm{d}s} \xrightarrow{d} N(0,1). \tag{28}$$

Note that we use the threshold pre-averaged BV to form the jump t-statistic. To obtain a feasible limit theorem, we substitute the integrated variance appearing in the denominator with $BV_N^*[Y](\tau)$.

The results on size and power are reported in Figure 4 for a subset of the simulated models. Panels A and B uncover the size properties of the above t-statistic for model BM and SV2F. In model BM, the actual fraction of rejections is close to the nominal size of the test for all choices of θ and the distribution looks close to Gaussian. Turning next to model SV2F, the standard normal still offers a good description of finite sample variability of the t-statistic, but we note a slight size distortion when $\theta = 0.1$. Although the distortion shrinks as θ increases, it does not vanish completely. Under model SV2F, the path of volatility is very erratic and some part of the size distortion is undoubtedly related to the fact that we are setting a global threshold in our computations, which depends on a constant measure of variance, rather than a local, spot estimate of volatility. However, although in principle it is straightforward to extend the threshold theory to allow for a time-varying barrier, it requires highly non-trivial computational efforts compared to the small gains associated with it. Therefore, we do not venture down this path here.

In Panel C–D, we inspect the rejection rate of the test in the presence of jumps using model BMJ. The following conclusions can be made. First, in Panel C we see that already by the time $N = 10,000$, the simulated power of the test is good and lies in the range of about 65 – 77%, depending a bit on the specific choice of θ. Again, $N = 10,000$ is a conservative sample size for our ultra high-frequency milli-second data employed in the empirical section. Indeed, as shown in the web appendix, model BMJ has the weakest power amongst all the jump-diffusion models considered. Nonetheless, there is a tendency for power to drop as K increases, so the results caution against using too extreme values of θ in practice. Second, Panel D conducts a sensitivity analysis by showing the distribution of the log-based jump t-statistic, when we surpass the thresholding step. As evident, this has a pernicious impact on the rejection rate caused by two complementary factors, as detailed in the upper right-hand corner of each subpanel. There, we report the average

Figure 4: Log-based jump t-statistic – Size and power.

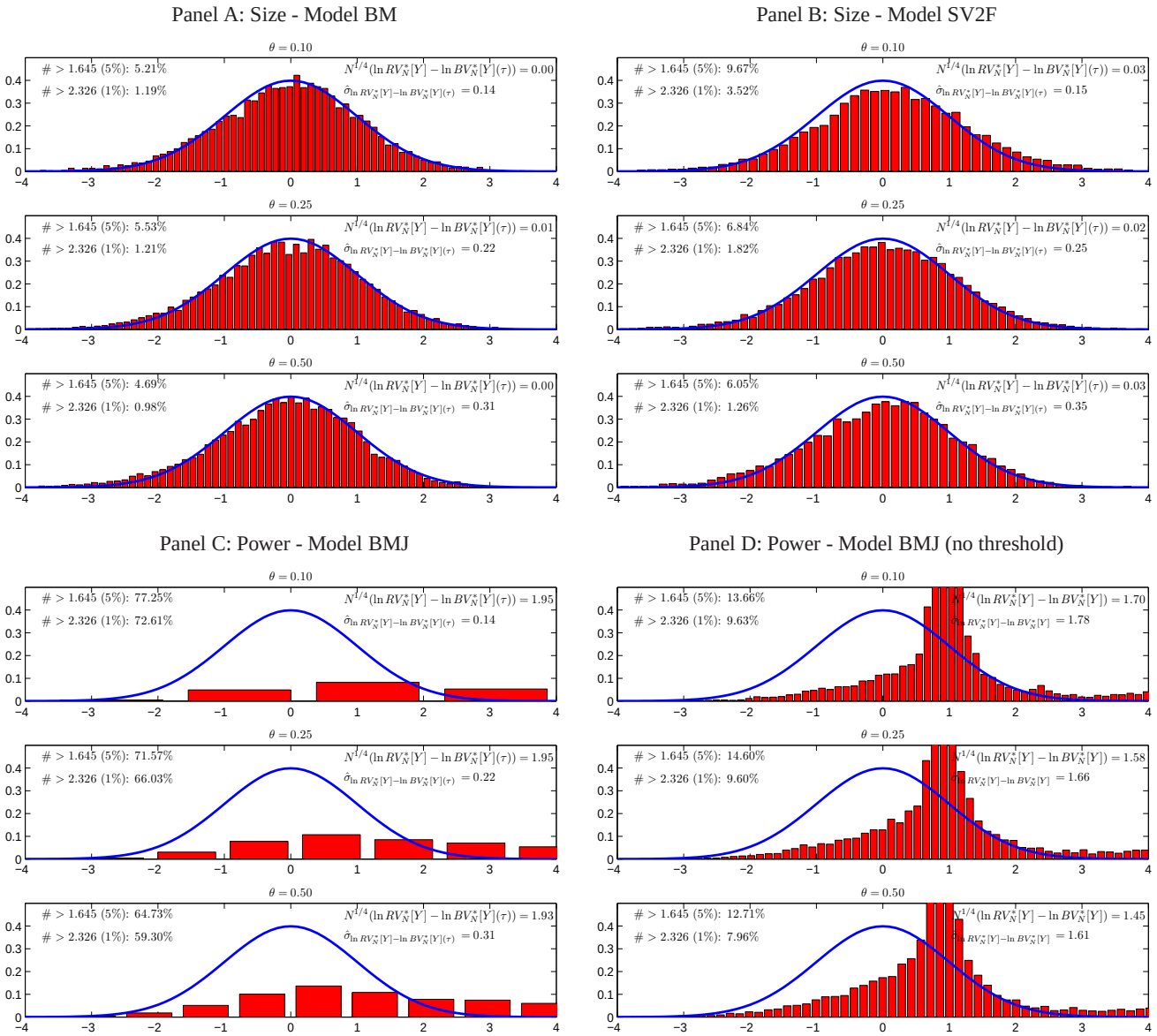

Note. The histograms show the simulated distribution of the log-based jump t-statistic defined by Eq. (28) using $\theta = \{0.10; 0.25; 0.50\}$. In the upper left-hand corner of each subpanel, we report the fraction of t-statistics that exceed the $1-$ and $5-$ % critical value in the right tail of the standard normal distribution. To the right, we show the average value of the numerator and denominator across the $10,000$ repetitions. The density function of the standard normal is superimposed for reference.

value of the numerator and denominator of Eq. (28). The first factor is the upward bias in the pre-averaged BV revealed above, which depresses $N^{1/4}(\ln RV_N^*[Y] - \ln BV_N^*[Y])$. The second is buried in the construction of our block subsample covariance matrix estimator, which is sensitive to jumps in finite samples, when the number of subsamples d is small. If

one of the subsample estimates deviates from the rest due to the presence of jumps, this will cause a significant increase in the sample variation of the subsampled RV and BV. This produces a large upward bias in $\hat{\Sigma}^*$, which in the end deflates the t-statistic. Thus, it appears crucial to use the threshold filter in practice to preserve power.

4 Empirical application

In this section, we use the pre-averaged RV and BV measures to provide an in-depth study into the role of the jump component for a representative set of US equity and foreign exchange rate data. To the best of our knowledge this is the first study to take a comprehensive look at the magnitude of the jump variation component as measured from noisy tick data sampled at ultra-high frequencies. We also report results based on 5- and 15-minute sampling frequencies as these are widely used in the literature and provide a natural reference point.

4.1 Data description

We have available a large set of tick data covering a representative set of foreign exchange rates and large cap US equity and US equity-index data. The sample period is from January 2007 through to March 2011 (or 1170 trading days) and includes several episodes of exceptional turbulence such as the global housing and credit crisis, the S&P500 flash-crash, the European sovereign debt crisis and the bail-out of Greece, and the Japanese earthquake.

For the equities, we consider all thirty Dow Jones Industrial Average (DJIA) index constituents as of October, 2010, as well as two market-wide indices traded as highly liquid ETFs, namely QQQ tracking the NASDAQ100 index and the SPY (or spiders) tracking the S&P500 index. The latter one is included because it is used in many other studies (see Table 1) and thus provides a good benchmark. The data is extracted from the NYSE TAQ database, and includes both quote and trade data with milli-second precision time-stamps allowing for a very fine grained view of the price evolution. We restrict attention to the official trading hours from 9:30 - 16:00 local New York time.

For the foreign currency data, we have the three major rates of Euro, Japanese Yen, and Swiss Franc all traded against the US dollar, i.e. EURUSD, USDJPY, and USDCHF, respectively. The data comes from the EBSLive data feed that also provides both trade and quote data with milli-second time-stamps. We restrict attention to the most liquid London and New York trading hours from 7:00 - 19:00 (GMT).

We pre-cleaned the data following the routines proposed in Barndorff-Nielsen, Hansen, Lunde, and Shephard (2009), and compute all results both on trade and (mid-) quote data. After cleaning, we are looking at a total sample size of well over 4 billion observations! To conserve space, we only report the results for the trade data.

Table 3: Jump variation estimates for equity and FX high-frequency data.

			tick frequency			5-minute frequency			15-minute frequency		
	N	γ	RV^*	BV^*	JV	RV	BV	JV	RV	BV	JV
Panel A : Equity indices											
QQQ	48,336	0.38	22.8	23.0	-1.6	22.8	22.4	3.7	22.7	21.6	8.9
SPY	112,921	0.35	21.1	21.2	-0.3	20.9	20.5	4.1	20.7	19.8	8.1
Panel B : Individual stocks											
AA	31,263	0.51	48.4	48.0	1.7	48.9	47.6	5.1	47.2	44.8	9.9
AXP	31,205	0.27	46.7	46.3	1.6	46.6	45.0	6.9	45.8	43.2	11.0
BA	20,961	0.26	30.5	30.3	1.5	30.5	29.4	6.5	30.4	28.5	11.8
BAC	82,426	0.82	59.0	59.3	-0.8	58.9	56.2	8.9	58.2	54.6	11.8
CAT	27,227	0.25	36.6	36.6	0.4	36.6	35.6	5.3	36.2	34.6	8.8
CSCO	54,114	0.64	31.7	31.5	1.5	32.2	31.2	5.9	31.4	30.0	9.1
CVX	34,685	0.26	30.0	30.1	-0.6	29.6	29.0	4.6	28.7	27.4	8.9
DD	20,222	0.28	32.3	32.2	0.7	32.7	31.6	6.7	31.9	30.3	9.7
DIS	24,864	0.36	29.9	29.5	2.2	30.2	29.1	7.4	29.6	28.0	10.7
GE	56,107	0.76	38.2	38.0	1.0	38.2	36.6	8.0	38.1	35.4	13.6
HD	30,037	0.37	34.5	34.3	1.2	34.4	33.3	6.3	33.6	31.5	11.9
HPQ	35,482	0.33	29.8	29.3	3.2	29.8	28.9	6.2	29.0	27.1	12.1
IBM	25,173	0.26	26.0	25.9	1.1	25.4	24.6	6.3	24.7	23.2	11.6
INTC	54,601	0.65	32.1	32.0	0.6	32.4	31.2	7.4	31.3	29.3	12.5
JNJ	29,792	0.37	18.7	18.5	2.0	18.8	18.1	7.9	18.2	16.9	13.6
JPM	67,426	0.34	48.7	48.8	-0.4	48.5	47.2	5.3	47.8	45.2	10.8
KFT	20,451	0.44	22.8	22.3	4.6	23.1	21.9	9.8	22.1	20.5	13.9
KO	24,760	0.33	21.1	21.0	1.6	21.5	20.3	10.5	20.5	18.9	14.5
MCD	23,482	0.29	23.7	23.5	1.3	23.8	22.7	8.7	22.7	21.2	12.6
MMM	16,880	0.26	26.2	26.0	0.9	25.9	25.0	6.5	24.7	23.3	11.2
MRK	30,000	0.37	30.1	29.7	3.0	31.5	29.8	10.2	29.8	27.5	14.5
MSFT	59,840	0.59	28.3	28.2	0.8	28.3	27.4	5.8	27.5	25.7	12.1
PFE	37,371	0.81	26.5	26.2	2.2	26.7	25.6	8.4	25.5	24.0	11.2
PG	30,091	0.33	22.7	22.4	2.6	21.2	20.3	8.0	20.1	18.8	12.9
T	38,051	0.55	28.9	28.6	2.6	29.7	28.9	5.7	27.9	26.4	10.7
TRV	15,889	0.26	37.5	36.5	5.1	38.9	37.0	9.4	37.3	33.7	18.6
UTX	18,616	0.26	27.0	26.9	1.2	26.7	25.9	6.3	25.9	24.6	9.8
VZ	29,970	0.46	27.5	27.2	2.1	28.0	27.0	7.3	27.0	25.4	11.2
WMT	35,611	0.35	23.5	23.4	0.6	23.6	22.7	7.5	22.6	21.2	11.8
XOM	55,005	0.31	28.2	28.2	-0.3	27.7	27.0	5.1	26.8	25.5	9.9
Panel C : FX pairs											
EURUSD	22,483	0.48	9.9	9.9	-1.1	9.8	9.4	7.9	9.6	9.2	8.3
USDJPY	8,177	0.29	10.8	10.8	-0.3	10.8	10.3	9.4	10.4	9.8	10.0
USDCHF	4,357	0.35	10.4	10.3	1.7	10.7	10.2	9.5	10.4	9.8	11.0
Panel D : Cross sectional average by asset class											
Equities	38,214	0.41	31.0	30.8	**1.3**	31.1	30.0	**6.9**	30.2	28.4	**11.5**
Currencies	11,672	0.37	10.4	10.3	**0.1**	10.4	9.9	**8.9**	10.1	9.6	**9.8**

Note. The numbers printed in the table are time series averages computed across the sample period, which covers January, 2007 through March, 2011 (both included). N is the sample size, $\gamma = \sqrt{N\omega^2 / \int_0^1 \sigma_s^2 \mathrm{d}s}$ the noise ratio. The integrated variance is proxied by BV^* and ω^2 is estimated with $\hat{\omega}^2_{\text{AC}}$. Variational measures are reported as annualized standard deviation. Noise-robust estimators are based on $\theta = 1.0$. The relative jump variation (JV) is expressed in percent.

4.2 The magnitude of the jump variation component

The results below center around measuring the magnitude of the jump variation component, i.e the quantity defined in Eq. (3) and subject to numerous past studies. To compute this quantity from tick data, we estimate $[X]_1$ and $\int_0^1 \sigma_s^2 \mathrm{d}s$ as the average daily pre-averaged RV and BV measures as defined in Eqs. (15) – (16), respectively. To compute JV from low-frequency data, where the impact of noise is negligible, we use the standard RV and BV measures as defined in Eqs. (6) – (7) based on previous-tick sampling.

Table 3 reports the results for the two equity indices (Panel A), thirty individual equities (Panel B), three currencies (Panel C), and the cross-sectional averages by asset class (Panel D). The single most important observation to be made is that the estimated jump variation computed from tick data is small. Much smaller than what is computed from 5- or 15-minute data and much smaller than what is reported by the extant literature as summarised in Table 1. The cross-sectional averages by asset class convey the message most clearly: using tick data we find that jumps account for a mere 1.3% of total return variation for equities and a negligible 0.1% for currencies! The corresponding figures for the widely used 5- (and 15-) minute sampling frequency are in line with the literature at a much more substantial 6.9% (11.5%) and 8.9% (9.8%) for equity and FX data, respectively. It is also interesting to note that for each asset there is a strict ordering in JV by sampling frequency where the tick data gives the lowest (and we argue most accurate) value and the 15-minute data the highest.

The results in Table 3 use a pre-averaging parameter of $\theta = 1$. To show that our results are robust to this choice of tuning parameter consider Figure 5. Panels A and B report the cross-sectional average of the annualized (estimated) standard deviation, as a function of θ ranging from 0.1 to 2.0, for the noise-robust RV and BV, the latter both with and without threshold elimination. As a reference point, we also report the corresponding levels of volatility estimated via the low-frequency RV_{5m} and BV_{5m}. Consistent with the findings of Hautsch and Podolskij (2010), we see that the pre-averaging estimators produce a pronounced, systematic downward bias if the selection of θ is too low to fully obliterate the impact of microstructure noise. Here, that interval appears to be roughly 0.1 – 0.5. For values of θ above 0.5, the estimated levels of volatility are fairly stable around 30% and 10% for equity and FX respectively, with $RV_N^*[Y]$ and the jump-robust estimators tending to track each other quite closely. We should note that threshold elimination has only a modest effect on the estimated level of volatility, suggesting that "large" jumps are relatively infrequent. Panels C and D of Figure 5 draw θ-signature plots – the estimated jump variation against values of θ – and indicate good robustness of our main finding. In particular, for values of θ above 0.5 the estimated JV is very stable and in a tight range of 1% to 2% for equity data and -0.5% to 0.5% for FX data.

Next, to show robustness of our finding over time Figure 6 plots the JV for the equities and currencies by calendar

Figure 5: θ-signature plot of annualized volatility and jump proportion.

Panel A: Annualized volatility, equity data

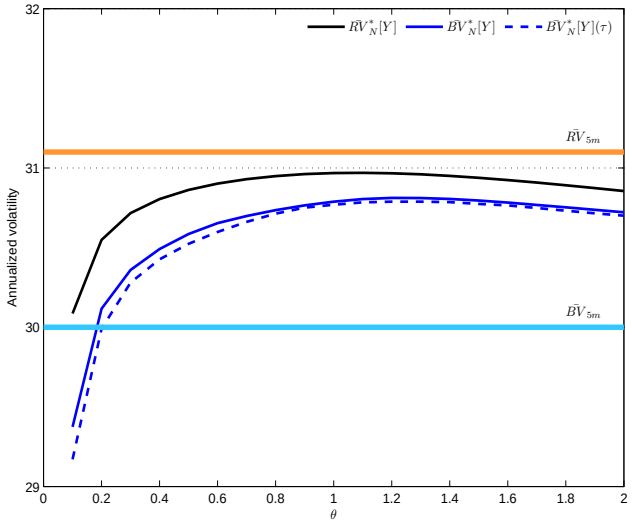

Panel B: Annualized volatility, FX data

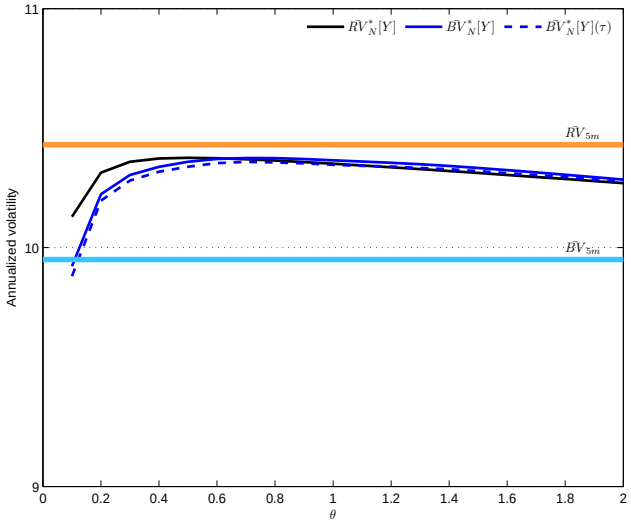

Panel C: Jump proportion, equity data

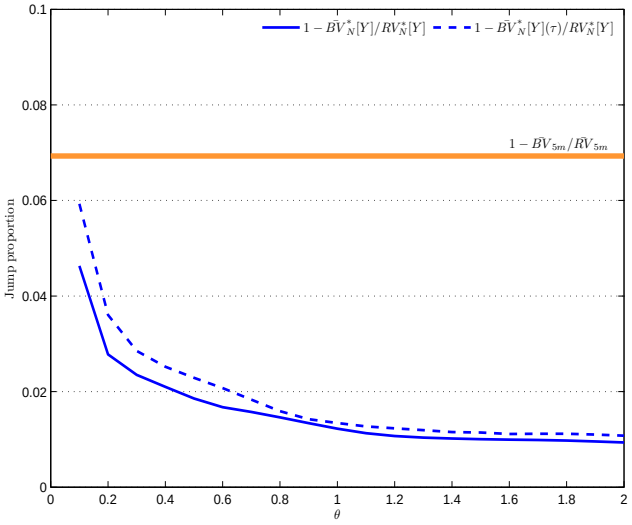

Panel D: Jump proportion, FX data

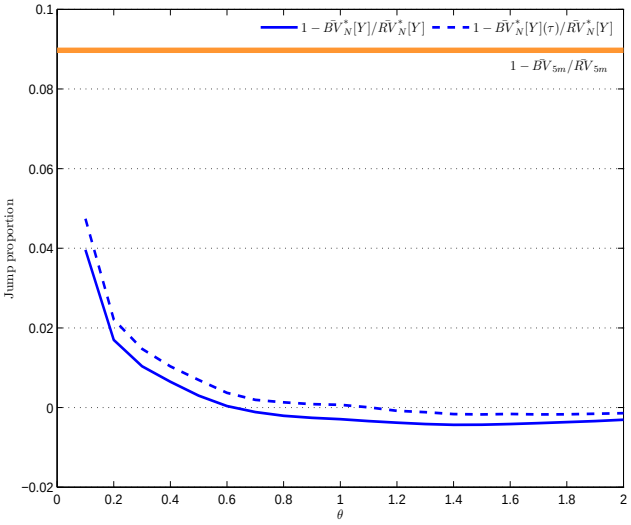

Note. In the upper row, we report the average annualized volatility of the noise-robust estimators, averaged across the cross-section of stocks and FX pairs included in our empirical application, as a function of θ in the range 0.1 – 2.0. As a comparison, we also show the average value of RV_{5m} and BV_{5m}. In the bottom row, we create a θ-signature plot for the estimated jump proportion using two different jump-robust pre-averaging statistics. Here, as a reference, we report the jump proportion inferred by RV_{5m} and BV_{5m}.

quarter over the full four year sample period. The dashed lines indicate the full-sample average for reference. The main observation to make here is that the results are stable, i.e. the estimated jump variation from tick data is consistently very small for equities (never exceeding 4% on any given quarter) and negligible for currencies. Also note the low-frequency

Figure 6: Jump proportion, quarter-by-quarter.

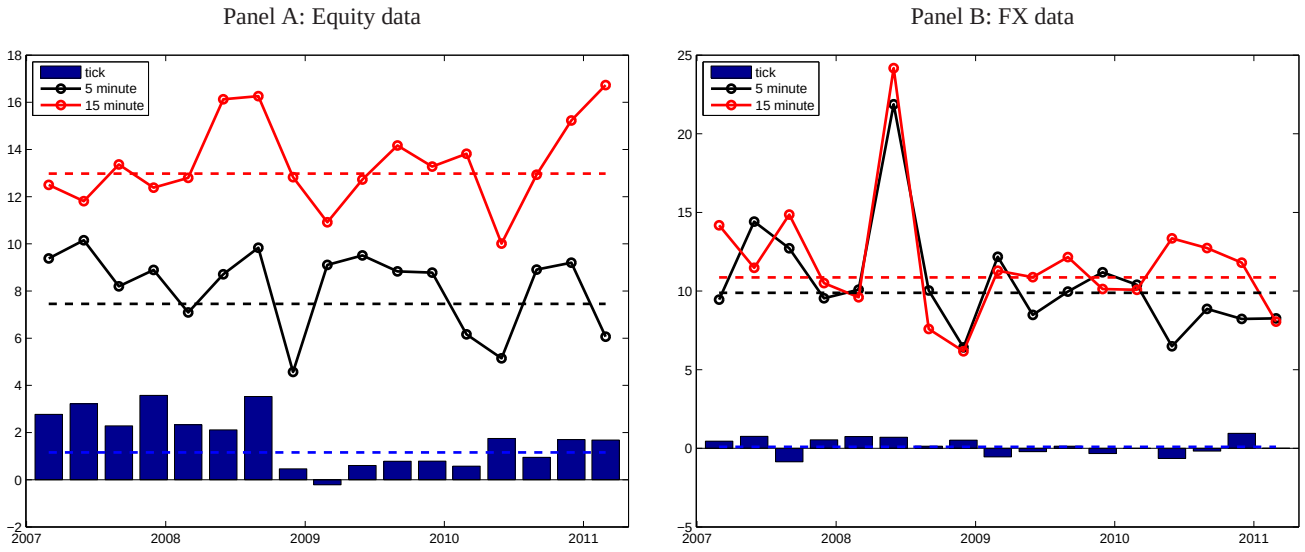

Note. We plot the estimated jump proportion, quarter-by-quarter, from Q1, 2007 through Q1, 2011 using ultra high-frequency estimators (tick) and low-frequency estimators based on 5- and 15-minute previous-tick sampling.

estimates always lie strictly above the tick estimates with highs of around 15% and 20% for equities and FX.

A nice way of summarizing our results for the whole sample are depicted in the scatter plots in Figure 7. In Panel A-B, we show the threshold pre-averaged BV plotted against the pre-averaged RV using $\theta = 1.0$. It is evident that the pairwise observations scatter closely around the 45-degree line. To highlight this, we run a regression, where the jump-robust estimator is projected onto the measure of total return variation. In Panel A-B, the regression equation is $BV_N^*[Y](\tau) = b_0 + b_1 RV_N^*[Y] + \epsilon$, which yields OLS coefficient estimates of $\widehat{b}_0 = -0.061$ and $\widehat{b}_1 = 1.002$ for the equity data and $\widehat{b}_0 = -0.000$ and $\widehat{b}_1 = 1.000$ for the FX data. To strengthen the analysis, we carry out a test of the hypothesis $b_0 = 0$ and $b_1 = 1$. In our setting this essentially amounts to asking, if on the average the data are compatible with being generated from a model without jumps. As seen in the subpanels, the test statistic $t_{b_1=1}$ is borderline significantly different from unity for the equity data, while there is no evidence in favor of rejecting the null using any of the other test statistics. By stark contrast, in Panel C-D the cloud of observations is much more skewed underneath and to the right of the 45-degree line, and when we run the regression $BV_{5m}[Y] = b_0 + b_1 RV_{5m}[Y] + \epsilon$, it results in intercept and slope coefficient estimates of $\widehat{b}_0 = 0.026$ and $\widehat{b}_1 = 0.925$ for the equity data and $\widehat{b}_0 = 0.022$ and $\widehat{b}_1 = 0.859$ for the FX data. It should be pointed out that the estimate of b_1 for the equity data matches closely with the jump proportion of roughly 7% that was discovered above in Table 3, while the slope coefficient for the FX data is somewhat lower than what is implied by the jump proportion above. The test statistic $t_{b_1=1} = -5.21$ and $t_{b_1=1} = -4.47$ leads to a clear rejection of

Figure 7: Regression analysis.

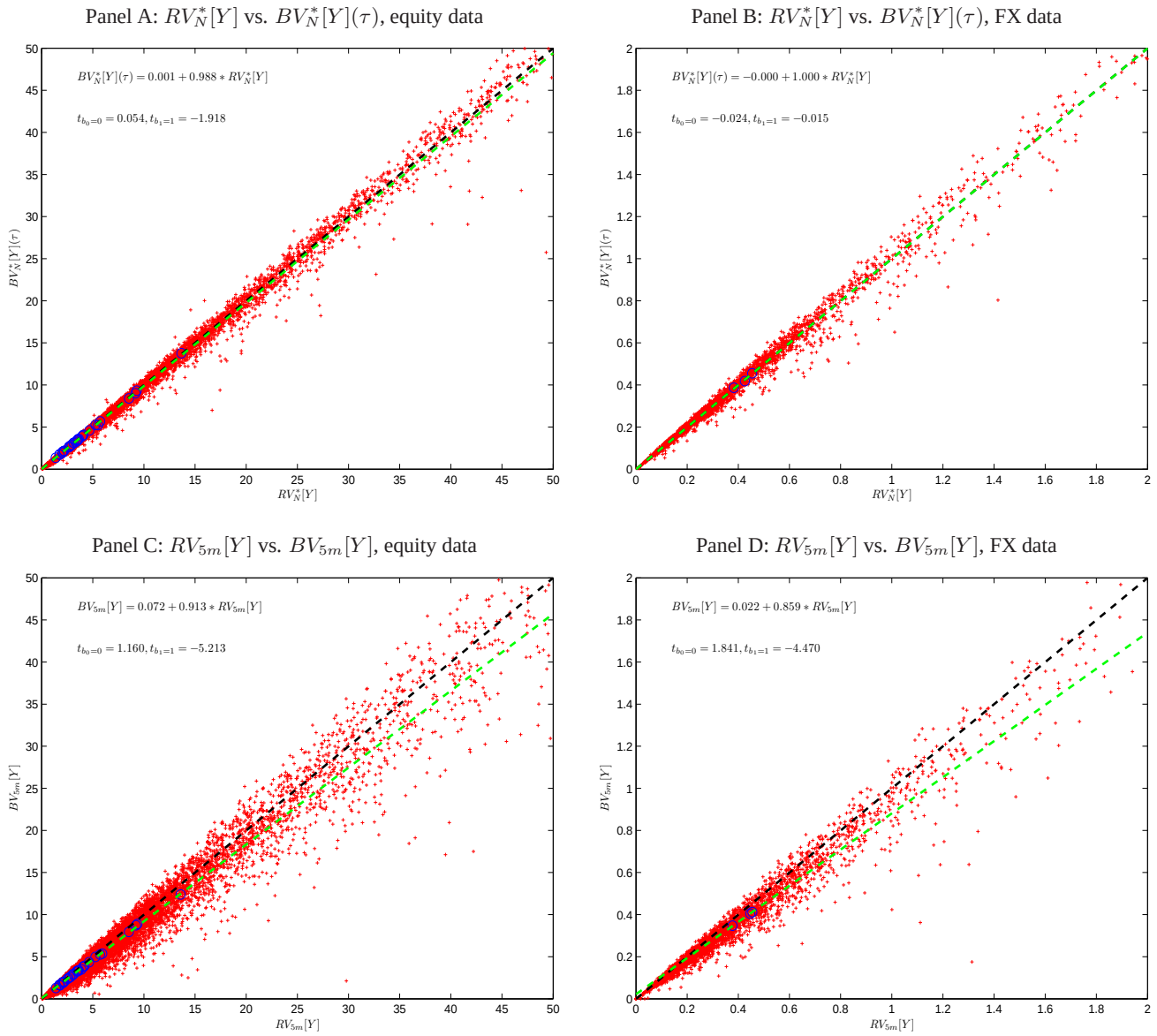

Note. The plot shows pairwise values of RV and BV. Upper panels are based on noise-robust pre-averaging estimators, while the lower panels are based on 5-minute low-frequency data. A red plus (+) marks a daily pairwise observation for each ticker in our selection of stocks and fx pairs. The blue circles (**o**) show the time series average value of RV and BV for an individual security. We fit a regression line to the values of RV and BV and conduct a test of the hypothesis $b_0 = 0$ and $b_1 = 1$ (t-statistics based on White's heteroscedasticity-consistent standard errors are reported in subpanels).

the null hypothesis, thus showing that even after adjusting for sampling uncertainty, BV_{5m} remains significantly smaller than RV_{5m}.

4.3 Significance testing

To attach a measure of significance to our daily estimates of jumps, we again implement the noise-robust jump test defined by Eq. (28) by selecting a block length of $L = 5K$ and construct $d = 20$ subsample estimates of the pre-averaged RV and BV.[12] We base the 5-minute low-frequency jump test on the modified ratio-statistic (with maximum correction), as advocated by Barndorff-Nielsen and Shephard (2006) and Huang and Tauchen (2005), where $\int_0^1 \sigma_s^4 \mathrm{d}s$ is estimated with the realised quadpower quarticity statistic.

Table 4: Significant jump days of equity and FX high-frequency data.

	$z_{RV^*_N[Y]}(A)$	$z_{RV_{5m}}(B)$	$A \cap B$		$z_{RV^*_N[Y]}(A)$	$z_{RV_{5m}}(B)$	$A \cap B$
Panel A : Equity indices				*Panel B (cont'd)*			
QQQ	6	113	0	MCD	27	179	5
SPY	28	118	5	MMM	29	159	10
				MRK	42	204	13
Panel B : Individual stocks				MSFT	51	162	8
AA	20	140	4	PFE	65	191	23
AXP	27	145	6	PG	35	163	6
BA	21	168	6	T	59	185	21
BAC	36	141	7	TRV	47	158	12
CAT	14	120	2	UTX	21	150	6
CSCO	66	152	12	VZ	31	173	10
CVX	13	113	2	WMT	16	174	6
DD	28	151	7	XOM	16	123	3
DIS	42	164	11				
GE	50	161	9	*Panel C : FX pairs*			
HD	25	147	6	EURUSD	12	122	5
HPQ	42	155	13	USDJPY	5	139	2
IBM	28	165	6	USDCHF	23	110	5
INTC	29	168	10				
JNJ	42	190	11	*Panel D : Cross sectional average by asset class*			
JPM	14	111	2	Equities	33	158	8
KFT	64	213	16	Currencies	13	124	4
KO	30	185	7				

Note. We report the number of rejections flagged by the individual jump test-statistics (out of 1170 days). All numbers are computed at the 1-% level of significance. The intersection ($A \cap B$) is defined as the number of days with jump signals in common.

Table 4 holds the outcome. As expected, we see that the noise-robust jump test, $z_{RV^*_N[Y]}$, has substantially fewer significant jump days compared to the low-frequency 5-minute version, $z_{RV_{5m}}$, which mirror images the results on jump proportions above. On average, $z_{RV_{5m}}$ signals the appearance of jumps by a factor 5 – 10 relative to $z_{RV^*_N[Y]}$.[13] In reality, we believe jump proportions are even smaller and that there are fewer significant jump days than what our noise-robust

[12]The sole exception is the USDCHF cross, which is based on $d = 10$ subsamples. This is because for the USDCHF, the total amount of data at our disposal is often insufficient to get reliable covariance matrix estimates using $d = 20$ subsamples.

[13]Note that some of the rejections in Table 4 merely reflect the choice of significance level, α, inducing on average αT false rejections of the null

ultra high-frequency jump test suggests, because many of the jump signals we investigated by manual inspection appear not to be real jumps, but we will dig deeper into this discussion in Section 6.

4.4 The burst of volatility hypothesis

The results reported so far all point towards a much reduced role for jumps in explaining the total return variation for equity and currency data. Indeed, we find that the jump variation computed from tick data is an order of magnitude smaller than the consensus view of a very substantial body of literature that uses 5-minute or lower frequency data. How can these findings be reconciled?

A plausible explanation is that our ability to tell true *discrete* jumps from *continuous* diffusive variation diminishes, as we lower the sampling frequency, N. Specifically, it is likely that a short-lived burst of volatility is mistakenly identified as a jump with less frequent sampling. The flash-crash episode discussed in the introduction is a prominent example of such a scenario. The Japanese earthquake provides another for the currency data. Figure 8 plots the evolution of the USDJPY rate in Panels A and B for the period in question. From the 5-minute data, two very substantial jumps are evident. One, on March 16, when a panicked USDJPY sell-off led to a "flash-crash" type drop in the rate and one, on March 18, on a coordinated central bank intervention aimed at devaluing the JPY. Panels C and D draw the tick data for the respective episodes and tell a very different story where price jumps remain elusive. Searching through the full sample period and all the 35 securities considered here, we confirm this "burst of volatility" pattern is the dominant explanation for the much reduced role of jump variation.

To provide some additional support for the burst of volatility conjecture, we consider a simple simulation study. In particular, we draw noise-free prices from a scaled Brownian motion, $\mathrm{d}X_t = \sigma_t \mathrm{d}W_t$ for $t \in [0,1]$, where $\sigma_t = 5\sigma^*$ for $t \in [16/32, 17/32]$ and $\sigma_t = \sigma^*$ otherwise, where σ^* is fixed at a level corresponding to 40% in annualized terms. In this scenario, σ_t is piecewise constant and increases five-fold in strength over a short interval of the day (equivalent to a 15-minute interval based on an 8-hour trading session), thus creating a jump in volatility, but there are no jumps in the price, implying that the true jump variation is zero. We simulate noisy log-prices as above, $Y = X + u$, using i.i.d. noise with a noise ratio parameter of $\gamma = 0.5$ and then round Y to the nearest cent to induce price discreteness, based on a starting price of \$50 in levels. Finally, we construct the low-frequency RV and BV at varying sampling intervals and calculate the average jump variation across 10,000 simulation trials.

Figure 9 illustrates our findings using a signature plot that draws the measured jump variation as a function of sampling frequency on a log-log scale. Panel A is based on the above simulated data, and we see quite clearly that the jump variation is severely inflated at lower sampling intervals, but that it steadily drops as we move from half-hourly sampling

hypothesis, where T is the number of days in the sample.

Figure 8: USDJPY earthquake episode: Jump or burst in volatility?

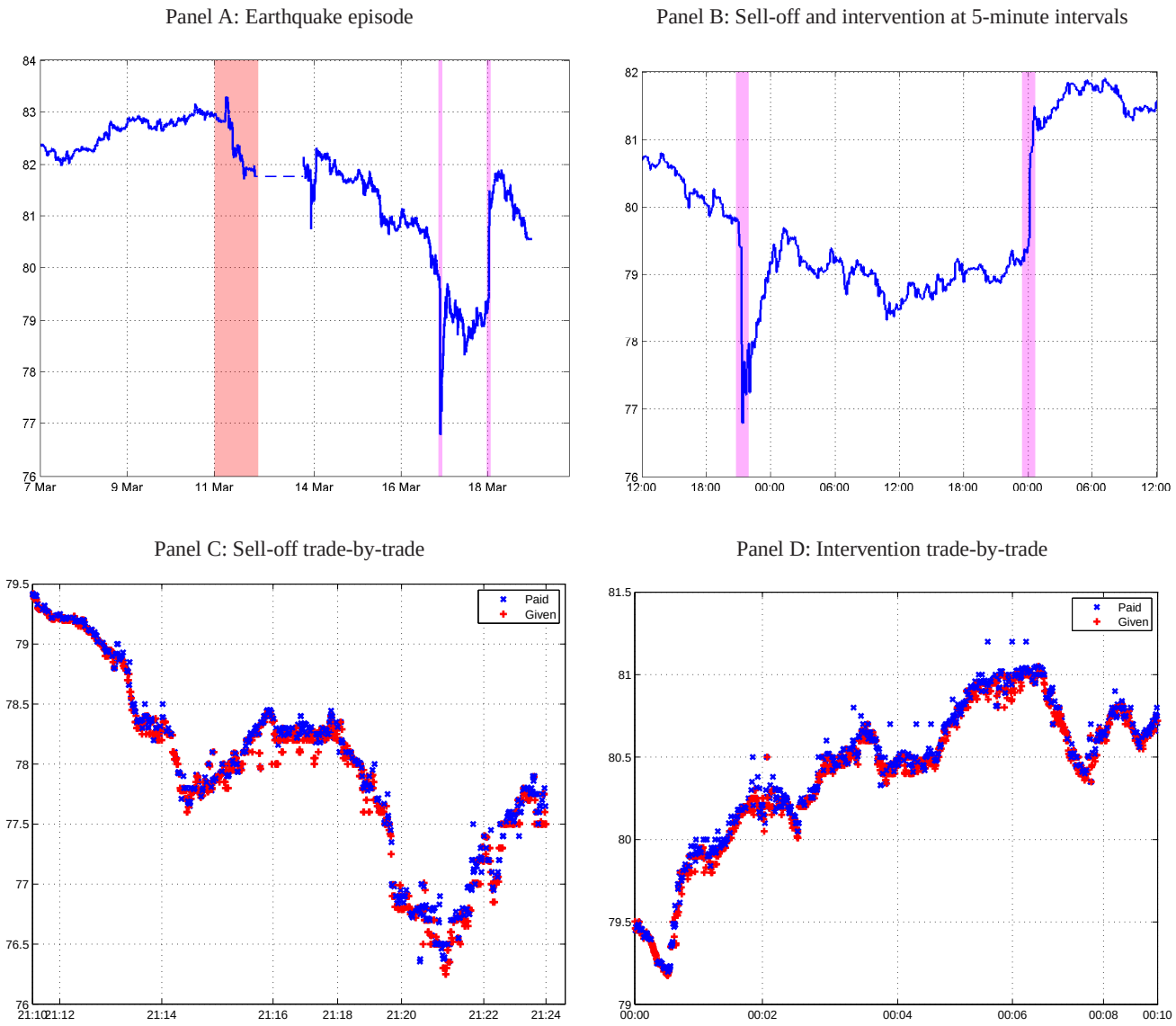

Note. EBSLive USDJPY spot data for March 7 – 18, 2011 with time reported in GMT. "Paid" and "given" denote aggressive buy- and sell-orders, respectively.

to 2-minute sampling. Beyond this point, the microstructure noise kicks in and the traditional statistics inflate the jump variation again, as the sampling frequency increases further. Panel B of the figure plots the corresponding results for the cross-sectional average of the full sample of equity instruments. The results are strikingly similar to the simulation-based evidence, thus reinforcing and supporting the burst of volatility hypothesis.[14] Note that, by contrast to the low-frequency

[14]The jump variation signature plot for the foreign exchange rate data display a similar, but less pronounced, U-shape. Because we are only

estimators, our pre-averaged noise-robust jump variation measures can be applied to tick data and doing this we observe a jump variation ending up at around 1% for the equity data. Interestingly, this closely coincides with the trend conveyed by the conventional statistics based on the infeasible noise-free data in Panel A of Figure 9.

Figure 9: Jump variation signature plot.

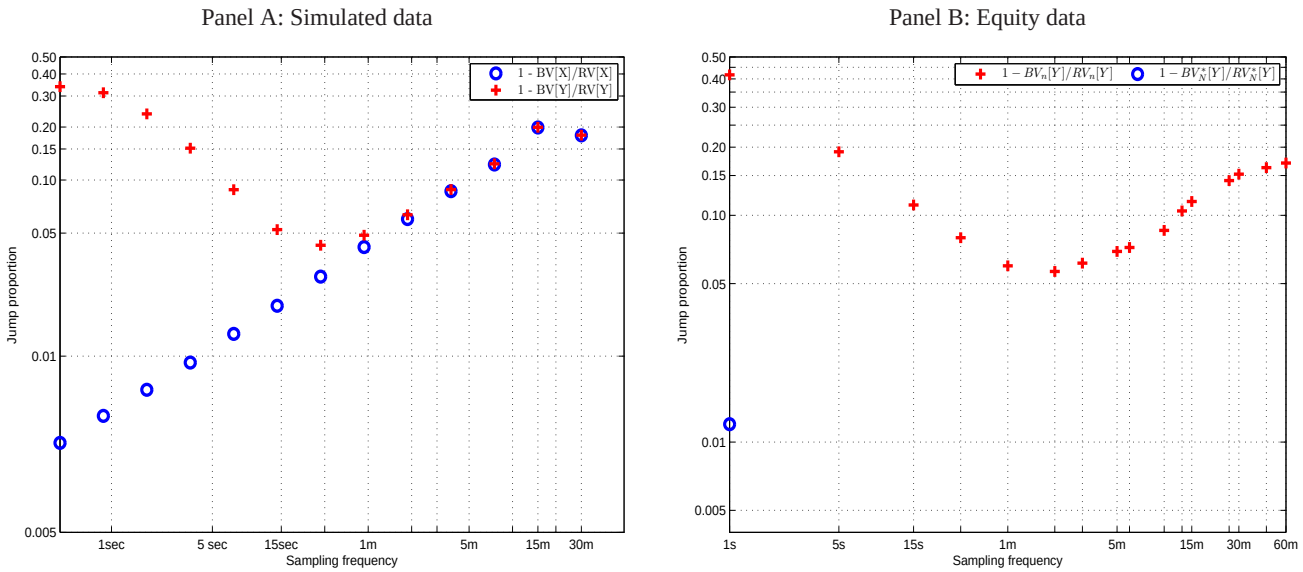

Note. Average jump variation estimates as a function of the sampling frequency. Left panel is based on simulated data, while the right panel covers the full sample of equity instruments (both cross-sectionally and over time). The red plus marks (+) denote the estimates based on noisy prices by comparing the standard RV and BV measures (which are not valid in the presence of noise). In Panel A, the blue circles (**o**) denote the infeasible jump variation computed from the noise-free prices, while in Panel B it indicates our noise-robust jump variation estimate based on tick data.

Finally, to shed some theoretical light on the above hypothesis, we obtain the following expression for the unconditional bias of BV (see Appendix A for assumptions and the derivation):

$$E\left(BV_N[X] - \int_0^1 \sigma_s^2 \mathrm{d}s\right) = -\frac{1}{N} E\left(\frac{1}{12}\int_0^1 \frac{\upsilon_s^2}{\sigma_s^2}\mathrm{d}s\right) + o(N^{-1}), \tag{29}$$

where υ is the "volatility of volatility".

Based on this expression, we learn that with time-varying volatility, and in the absence of noise, (i) $BV_N[X]$ is downward biased in finite samples, translating into an inflated JV measure, (ii) the effect is stronger with a high volatility of volatility υ or a lowering of the sampling frequency N. Stated differently, a short-lived burst of volatility may spuriously be attributed to the jump variation component and this mistake is increasingly likely as the sampling frequency of the data is lowered. This line of thought is also consistent with Aït-Sahalia and Jacod (2009c), who emphasize that jumps can only

considering three FX pairs, there is less averaging taking place, which could explain the less clear-cut pattern.

be identified by increasing the sampling frequency to the limit, which is what this paper does and leads us to argue for a much reduced role of jumps (and by implication an elevated role of the volatility process).

5 Illustrative example: Option trading with rehedging

In this section, we briefly illustrate the economic relevance of the above finding using an option pricing example (portfolio allocation and risk management are two other areas of finance, where our findings have profound implications). Specifically, we consider a scenario where a market maker providing liquidity in short-term at-the-money call options gets paid on a quote one day before maturity of the contract. As a result of this trade, the market maker is now short the call option and decides to remove the first order price risk by covering the delta of the position using the underlying instrument.[15] To maintain a simple setting, we simulate log-prices from a scaled Brownian motion with no drift: $X_t = \sigma W_t$, and we price the option with the Black-Scholes formula.[16] σ is fixed at 40% in terms of annualized volatility. The number of steps in each simulation is $N = 1,000$ and we generate a total of 10,000 independent price paths. The initial equity price is set to 100, which also equals the strike price of the call option. As already mentioned, the option has one day left to maturity and expires at the end of trading, where the position is settled. The equity pays no dividends during this time. The risk-free rate is set to zero.

The market maker receives a premium for selling the option and is initially delta neutral because of the hedge, but he is left short gamma and accumulates losses that are proportional to the square of the change in price of the underlying. Of course, in a perfect, frictionless market, the trader can replicate the option by continuously rehedging, and the premium will exactly offset the losses associated with his rebalancing activities. However, market microstructure noise induces transaction costs, so we assume our imaginary trader has decided to rehedge his equity exposure only after every 50 basis point move in the underlying. At each rebalancing, a small loss is locked in due to the negative gamma profile. At expiry, if the option is in-the-money, the equity is delivered to the buyer and a further loss is taken, else the option expires worthless and the market maker closes his position in the underlying at the prevailing market price. Finally, we keep track

[15] Writing a call option contract, while simultaneously purchasing a delta equivalent number of shares in the underlying stock is also known as a "buy-write" covered call strategy.

[16] The Black-Scholes call option pricing formula is given by: $C = N(d_1)S - N(d_2)Ke^{-rt}$, where S is the stock price, K is the strike, σ is the volatility, r is the risk-free rate, t is the time to maturity, $N(\cdot)$ is the distribution function of a standard normal random variate and

$$d_1 = \frac{\ln\left(\frac{S}{K}\right) + \left(r + \frac{\sigma^2}{2}\right)t}{\sigma\sqrt{t}}, \qquad d_2 = d_1 - \sigma\sqrt{t}.$$

The delta and gamma are defined as the first- and second-order derivative of C with respect to S and equal: $\Delta = N(d_1), \quad \Gamma = \frac{N'(d_1)}{S\sigma\sqrt{t}}$.

Figure 10: Simulated price path and P&L distribution.

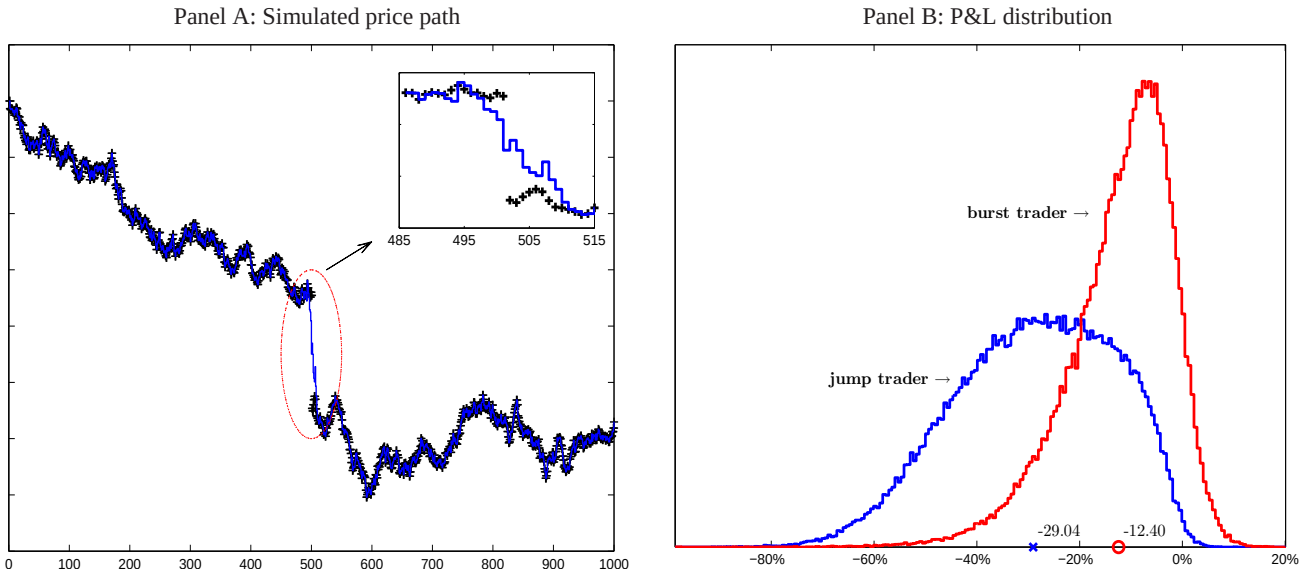

Note. In Panel A, we plot an example of simulated price paths for the option trader exercising the covered call strategy with rehedging. In Panel B, we show the distribution of his P&L and also report the average loss to the trader expressed in percent of the premium.

of the traders bank roll and calculate the total profit and loss (P&L) for the trade.

Now, in each simulation, at a random point in time, we hit the market with two forms of unforeseen news, which causes a revaluation of the stock. In scenario A, we place a 2% pure jump in price, while, in scenario B, we put a 2% "burst of volatility". The latter induces a swift, but continuous, change in price. Panel A of Figure 10 helps to highlight the distinction between these two types of shocks.[17] It shows an example of a simulated set of sample paths, and we provide an ultra high-frequency zoom on the price around the surprise move. As seen in the figure, and in contrast to a pure jump, scenario B provides the market maker with a valuable opportunity of rehedging his exposure, as the market declines. This shows up prominently in Panel B of the figure, where the distribution of the P&L is reported. Note that, because the realised volatility in X is larger than the volatility used for pricing the option, the trader loses money on average in both scenarios. A typical loss amounts to -29.04% and -12.40% of the premium charged in scenario A and B, respectively. Thus, not only is the average loss smaller for the "burst of volatility" trader, the distribution of his P&L is also less dispersed.

[17]Technically, the burst in volatility scenario is obtained by reconnecting the sample path in the jump scenario, using a Brownian bridge on the observations that lie 10 steps before and after the jump, as illustrated in the figure.

6 Robustness analysis: High-frequency data with outliers

In practice, tick data are often corrupted by outliers (e.g., due to delayed trade reporting, fat-finger errors, bugs in the data feed, misprints, decimal misplacement, incorrect ordering of data, etc). As a result, empirical researchers are often advised to build "pre-cleaning" algorithms that use systematic rules for filtering out suspicious observations. A prominent example is the Barndorff-Nielsen, Hansen, Lunde, and Shephard (2009) filter applied above. An obvious drawback of these filters is that they typically depend on underlying tuning parameters that control tolerance levels and the user consequently risks removing too much or too little data. In this section, we show that pre-averaging has an embedded robustness property against outliers and that pre-filtering of the data appears to be causing some of jumps we detect in practice.

To model outliers, we take

$$Y_{i/N} = X_{i/N} + u_{i/N} + O_{i/N}, \tag{30}$$

where, on top of the components defined above, $O_{i/N} = \mathbb{1}_{\{i/N \in \mathcal{A}_N\}} \mathcal{S}_i$. Here, $\mathcal{A}_N$ is a random set holding the appearance times of outliers, while their sizes are given by $(\mathcal{S}_i)_{i=1,\ldots,N_1^O}$. We assume that $\mathcal{A}_N$ is a.s. finite and model it by

$$\mathcal{A}_N = \left\{ \frac{[NT_i]}{N} : 0 \leq T_i \leq 1 \right\}, \tag{31}$$

where $(T_i)_{i=1,\ldots,N_1^O}$ are the arrival times of another counting process $N^O = \left(N_t^O\right)_{t\geq 0}$. In what follows, we assume that O is mutually independent of X and u, $O \perp\!\!\!\perp (X, u)$. This, in turn, implies that $N^J \perp\!\!\!\perp N^O$, i.e. the two counting processes generating jumps and outliers are also independent, which further means that the probability of observing both a jump and an outlier in a small time interval is asymptotically negligible.

Proposition 3 *Assume that Y follows Eq.* (30) *and that the conditions on X and u yielding the consistency and CLT of Proposition 1 are satisfied. Then, the conclusions of Proposition 1 are unchanged.*

Proof See appendix.

Compared to Section 2.3, Proposition 3 shows that pre-averaging estimators are, in addition to microstructure noise, also robust to the presence of finite-activity outliers. To give some intuition for this result, we assume that the diffusion part of X is zero. Then, almost all observations are i.i.d, except finitely many (which are also independent) that have a mean different from 0 (coming from outliers). An immediate consequence of this is that those finitely many outliers can not be statistically identified. At a more technical level, with probability approaching one, there is at most a single outlier in the window $[\frac{i}{N}, \frac{i+K}{N}]$. If present, the outlier influences two consecutive noisy returns, say $\Delta_{i+j-1}^N Y$ and $\Delta_{i+j}^N Y$. Therefore, it appears with a factor $O\Big(|g\Big(\frac{j}{K}\Big) - g\Big(\frac{j-1}{K}\Big)|\Big)$ in the construction of $\bar{Y}_i^N$, for some $1 \leq j \leq K$. But

Figure 11: Transaction price data for S&P 500 Depository Receipts (SPY), September 18th, 2007.

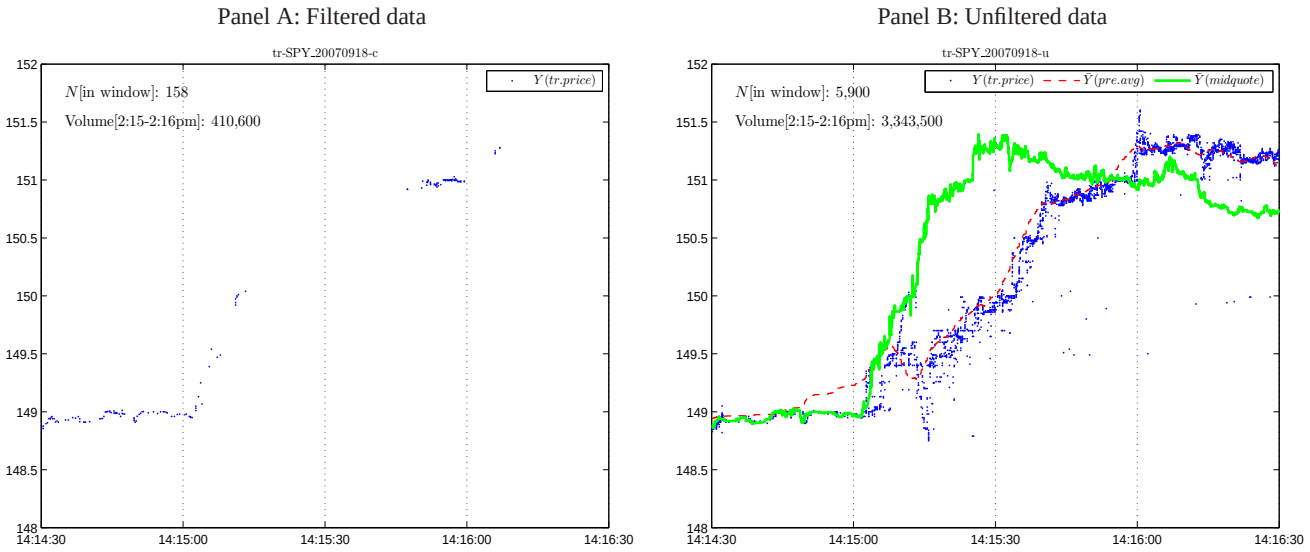

Note. The data plotted are transaction prices for SPY on September 18th, 2007. Panel A holds the filtered data, using the pre-cleaning rules of Barndorff-Nielsen, Hansen, Lunde, and Shephard (2009), while Panel B shows the raw data, as extracted from the TAQ database. The dashed, red line is the pre-averaging approximation of the efficient price, while the thick, green line shows the uncleaned midquote data.

$|g\left(\frac{j}{k_N}\right) - g\left(\frac{j-1}{k_N}\right)| = O(K^{-1})$ (uniformly), thus the impact of outliers on the pre-averaged returns is asymptotically negligible.

To demonstrate the potential of Proposition 3, we provide a practical example of what we term a "cleaning-induced" jump. To this end, consider Figure 11, which shows the cleaned and uncleaned transaction price data for SPY on September 18th, 2007 over the 2-minute window running from 2:14:30pm – 2:16:30pm.[18] At 2:15pm, the FED announced an unexpected rate cut of 50 basis points, in an attempt to shield the economy from the accelerating mortgage crisis. The stock market rallied upon receiving this news, moving the SPY higher from approximately index 149.00 to 151.25 in the following 60 seconds, equivalent to a log-return of about 1.5%. Looking at the cleaned data in Panel A, although some trading activity is observed in the 1-minute window from 2:15pm to 2:16pm, the move largely stands out as a pure jump in price. On this day, we compute an annualized value of $RV_N^*[Y]$ and $BV_N^*[Y]$ at 25.15% and 13.34%, respectively. Moreover, with the variance ratio $1 - BV_N^*[Y]/RV_N^*[Y]$ equal to 71.89%, it suggests that jump variation accounts for more than two-thirds of total variation and both the noise-robust and low-frequency jump test are in fact significant at the 1% level.

By stark contrast, a different story is told by looking at Panel B, which shows the raw data prior to cleaning, as they

[18]This day has also been highlighted as a significant jump day in a recent paper by Patton and Sheppard (2011).

are extracted from the TAQ database.[19] The red, dashed line in this plot is based on the pre-averaging representation in Eq. (14), which uses the next $K/2$ transaction prices to approximate the underlying, efficient price. Looking at this graph, the sample path variation instead appears to be a burst of volatility episode. But, it is clear that there are quite a few suspect observations in the data. Nonetheless, when we apply the pre-averaged RV and BV directly to the noisy, uncleaned data in Panel B, we now arrive at an annualized volatility of 17.40% and 17.35% for the $RV_N^*[Y]$ and $BV_N^*[Y]$ and our estimate of jump variation is very close to zero at 0.6%!

A genuine concern regarding the price appreciation seen in Figure 11 is that it was borne by a relatively illiquid market, in which traders were not able to intermediate. Indeed, the trade feed over the episode is substantially delayed relative to the quote feed. However, the illiquidity or non-tradeable market argument does not hold up. In fact, in the 1-minute interval following the announcement, the raw data feed reveals that a total of 3,343,500 shares of SPY exchanged hands, trading at all intermediate levels, and representing a notional value of about $500 million or more than 10 times the comparable average traded volume.[20]

Proposition 3 indicates the opportunity of weakening existing filtering rules and doing less aggressive data cleaning, when the processing of data is combined with the pre-averaging concept. It then induces some comfort in that even if you do not manage to build a "perfect" filter, you can effectively rely on pre-averaging to wipe out any leftovers in the data, as verified in our simulation section. Still, some pre-cleaning of data is advised in practice, because outliers can be so abundant or extreme that it takes too long for the asymptotics to kick in.[21] In addition, the assumptions behind the proposition do not cover all forms of outliers, although this can potentially be relaxed to some extent. Indeed, the above empirical results suggest that pre-averaging can accommodate data, which are seriously erroneous. However, at this stage we do not fully understand just how far this robustness property can be stretched, so we resist the temptation of performing a full-blown empirical analysis on uncleaned data. This will certainly be an interesting topic to study in future work.

[19] A large portion of the entries flagged for deletion in Figure 11 fall victim to the so-called (T4) rule of Barndorff-Nielsen, Hansen, Lunde, and Shephard (2009), whereby transactions are matched with trailing quotes. This suggests that the intensive trading in the aftermath of the FED announcement might have clogged the dissemination systems, and that a bulk of the subsequent trades were reported to the consolidated tape with some delay, making them appear out-of-line with current market conditions, as also indicated by the discrepancy between the midquote data and transaction prices in Panel B of the figure.

[20] The average daily 1-minute volume of SPY for the month of September, 2007 was 309,734 (352,192) shares based on the cleaned (uncleaned) high-frequency data, while the average volume for the 1-minute interval from 2:15pm – 2:16pm totalled 21,611 (175,974) shares.

[21] An example of this is March 5, 2007, where the high-frequency data for a number of companies in our analysis are severely disrupted. This day was also noticed by Andersen, Dobrev, and Schaumburg (2010), who developed additional filtering rules to handle it. In our empirical application, we decided to leave this day out of the analysis.

6.1 The noiseless case: $u = 0$

To the best of our knowledge, the addition of the outlier component is new to this paper, so here we complete this analysis by studying the marginal effect of adding outliers to the data, in the noiseless case: $u = 0$. As expected, the robustness property to outliers is not shared by the raw estimators in the noiseless case, as we now document. Note that, as we do not implement or otherwise use the results derived in this subsection, the investigation will be brief and focus solely on the theoretical side of things and not the practical aspects of their applicability.[22]

But, in this subsection,

$$Y_{i/N} = X_{i/N} + O_{i/N}, \tag{32}$$

for $i = 0, 1, \ldots N$.

To estimate and test for jumps in this model, we are going to need a third estimator, the so-called quantile-based realised variance (QRV hereafter) of Christensen, Oomen, and Podolskij (2010), which is defined in Appendix C.

Theorem 1 *Assume that there are outliers in the data but no microstructure noise, i.e.* $Y_{i/N} = X_{i/N} + O_{i/N}$*, where the process* X *follows Eq.* (1)*. Moreover, we assume that max* $(\lambda_j) < 1 - 1/m$*. As* $N \to \infty$*, it holds that*

$$\begin{pmatrix} RV_N[Y] \\ BV_N[Y] \\ QRV_N[Y] \end{pmatrix} \xrightarrow{p} \begin{bmatrix} 1 & 1 & 2 \\ 1 & 0 & \pi/2 \\ 1 & 0 & 0 \end{bmatrix} \begin{pmatrix} \int_0^1 \sigma_s^2 \mathrm{d}s \\ \sum_{i=1}^{N_1^J} J_i^2 \\ \sum_{i=1}^{N_1^O} \mathcal{S}_i^2 \end{pmatrix}. \tag{33}$$

Proof See appendix.

Remark 2 The condition $\max(\lambda_j) < 1 - 1/m$ in Theorem 1 means that $QRV_N[Y]$ discards at least the two largest absolute returns, which it requires to gain robustness to jumps and outliers.[23] It is of course possible to find multiple jumps and outliers in the data over small, but non-negligible, time intervals in practice. As discussed in Christensen, Oomen, and Podolskij (2010), we can control the finite sample robustness of the QRV to these joint effects by placing stronger restrictions on $\max(\lambda_j)$ and m. For example, suppose that there is an outlier *and* a jump in a small time interval, thus calling for the three largest increments to be removed. This can be achieved by taking $\max(\lambda_j) < 1 - 2/m$.

[22] Moreover, in practice when data are pre-filtered for outliers, it is typically rather unlikely to accidentally sample outlying returns, when low-frequency versions of the RV and BV are used to avoid the impact of microstructure noise, as in our empirical section. Hence, we really think of analyzing the impact on these estimators under the joint influence of noise and outliers using ultra high-frequency data and pre-averaging, as it was given above. Nonetheless, the results in this subsection are interesting from a theoretical point of view.

[23] As already pointed out by Christensen, Oomen, and Podolskij (2010), this excludes, for example, the so-called MinRV and MedRV of Andersen, Dobrev, and Schaumburg (2008), which are both special cases of the QRV.

To some extent, Theorem 1 is not surprising, as an outlier in the observed log-price Y translates into two consecutive jumps of roughly the same magnitude, but with opposite sign, in the return data $\Delta_i^N Y$. It implies that neither the RV nor the BV are consistent for the object, they are originally designed to estimate.

Moreover, even in the absence of jumps, $N_t^J \equiv 0$ for all t,

$$RV_N[Y] - BV_N[Y] \xrightarrow{p} (2-\pi/2)\sum_{i=1}^{N_1^O} O_i^2 > 0, \tag{34}$$

and thus a test for jumps based on the original RV and BV will reject the null hypothesis with a probability converging to one, if outliers are present in the data but unaccounted for. Indeed, we cannot estimate the jumps using only the RV and BV, which is why we need help from the QRV, because under the alternative of jumps

$$RV_N[Y] - BV_N[Y] \xrightarrow{p} \sum_{i=1}^{N_1^J} J_i^2 + (2-\pi/2)\sum_{i=1}^{N_1^O} O_i^2. \tag{35}$$

In order to estimate all three sources of empirical quadratic variation in this model, we proceed by inverting the matrix of coefficients appearing in Eq. (33) and use the resulting linear combinations of $(RV_N[Y], BV_N[Y], QRV_N[Y])$. The appropriate mix needed to estimate jumps is given by $RV_N[Y] - \frac{4}{\pi}BV_N[Y] - \left(1-\frac{4}{\pi}\right)QRV_N[Y] \xrightarrow{p} \sum_{i=1}^{N_1^J} J_i^2$, and this convergence is robust to the presence of finite-activity outlier processes by Theorem 1.

To conduct an empirical test for jumps, we need a joint distribution theory for the triplet of estimators under the null of no jumps or outliers. We present the CLT next, but, to ease the exposition, we concentrate on the QRV with a single quantile implementation $\bar{\lambda} = \lambda$.

Theorem 2 *Assume that $Y_{i/N} = X_{i/N}$, where X is a continuous semimartingale, i.e. X follows Eq.* (1) *but with $N_t^J \equiv 0$ for all t. Moreover, we assume condition (V) is fulfilled. As $N \to \infty$, it holds that*

$$N^{1/2}\begin{pmatrix} RV_N[Y] - \int_0^1 \sigma_s^2 \mathrm{d}s \\ BV_N[Y] - \int_0^1 \sigma_s^2 \mathrm{d}s \\ QRV_N[Y] - \int_0^1 \sigma_s^2 \mathrm{d}s \end{pmatrix} \xrightarrow{d_s} MN\left(0, \int_0^1 \sigma_s^4 \mathrm{d}s \times \Sigma\right), \tag{36}$$

where Σ is a 3×3 matrix with elements

$$\Sigma_{11} = \Sigma_{12} = 2, \qquad \Sigma_{22} = \frac{\pi^2}{4} + \pi - 3, \qquad \Sigma_{13} = \frac{m}{\nu_1^2(m,\lambda)}\mathrm{cov}\left((|U|_{(m\lambda)}^{(0)})^2, U_1^2\right)$$

$$\Sigma_{23} = \frac{\mu^{-4}}{\nu_1^2(m,\lambda)}\left((m-1)\mathrm{cov}\left((|U|_{(m\lambda)}^{(0)})^2, |U_1||U_2|\right) + 2\mathrm{cov}\left((|U|_{(m\lambda)}^{(0)})^2, |U_m||U_{m+1}|\right)\right)$$

$$\Sigma_{33} = \frac{1}{m}\Theta(m,\lambda) + \frac{2}{\nu_1^2(m,\lambda)}\sum_{k=1}^{m}\mathrm{cov}\left((|U|_{(m\lambda)}^{(0)})^2, (|U|_{(m\lambda)}^{(k)})^2\right),$$

where $U^{(0)} = \{U_i\}_{i=1}^{m}$, $U^{(k)} = \{U_i\}_{i=1+k}^{m+k}$, $\{U_i\}_{i=1}^{m+k}$ *is an independent standard normal sample and*

$$\Theta(m,\lambda) = m\frac{\nu_2(m,\lambda) - \nu_1^2(m,\lambda)}{\nu_1^2(m,\lambda)}.$$

Proof See appendix.

Finally, the only missing piece to perform a test for jumps is to exploit the linear combination given above, which is robust to outliers under the alternative, and then invoke the delta method on the joint asymptotic distribution in Theorem 2 to find the appropriate asymptotic distribution of the jump t-statistic under the null.

Remark 3 The integrated quarticity, $\int_0^1 \sigma_s^4 \mathrm{d}s$, appearing in the conditional variance of the limit distribution in Theorem 2 can be robustly estimated in the presence of jumps and outliers as outlined in Christensen, Oomen, and Podolskij (2010).

7 Concluding remarks

This paper uses new econometric techniques for separating out the diffusive variation component from the jump variation component, and applies these to a comprehensive set of tick data covering both equity and foreign exchange rate data to find evidence of a much reduced role for the jump component in explaining total return variation. Specifically, we find that the jump variation is an order of magnitude smaller than what is widely reported in the literature over the past four decades. The explanation for this can be found in the sampling frequency. The inability of the leading jump variation measures to account for market microstructure noise or market "friction" has prevented the literature from using tick data. Thus, in recent years a compromise 5-minute sampling frequency has been used. However, at this frequency we show that bursts of volatility are easily mistaken for jumps, thereby obscuring the "fact" that jumps are not nearly as common as generally thought. It goes without saying that a reduced role for jumps, and by implication an increased role for the volatility process, has many important implications for empirical finance applications such as option pricing, risk management, and portfolio allocation.

To conclude, we emphasize that price continuity as focused on in this paper is a rather narrow concept and that one may instead focus on "liquidity" as a more meaningful and insightful measure of market state. It is indisputable that markets are often subject to tremendous amount of stress. But we find this rarely leads to a substantial discontinuity in the price path at a milli-second tick resolution. Instead, what we do find is severe shocks to liquidity. Figure 12 illustrates this point using USDJPY data over the March 16, 2011 sell-off discussed above. Looking at the price path in Figure 8 we found little evidence of a price jump. Yet, from Panel A in Figure 12 we see that the inside spread which normally is

Figure 12: USDJPY liquidity shock over the March 16, 2011 sell-off.

Panel A: USDJPY spread

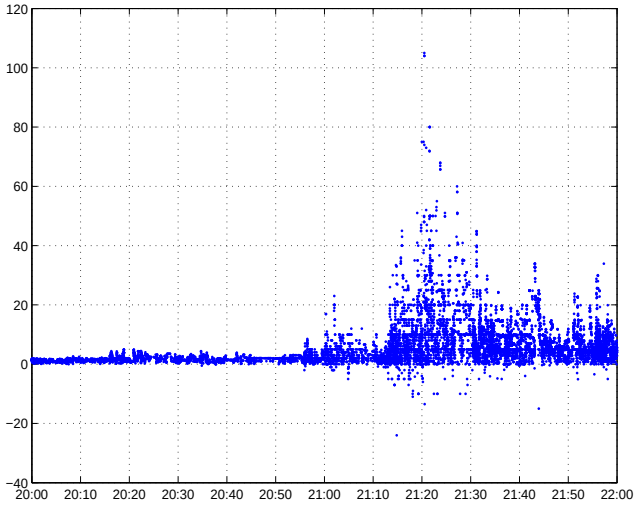

Panel B: Regular bid/offer quotes

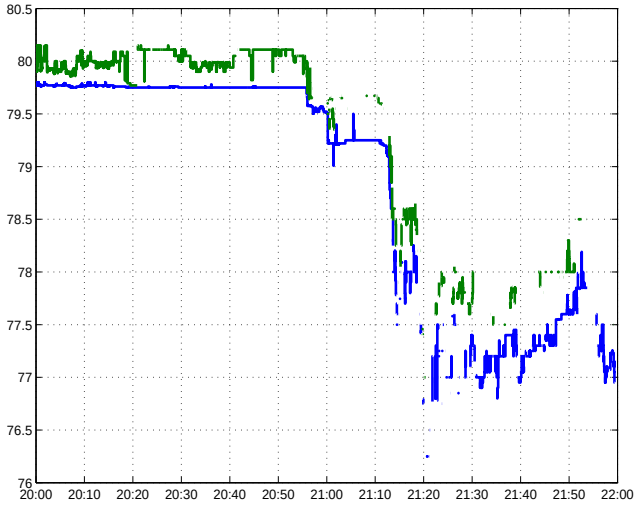

Note. Panel A reports the inside spread for USDJPY in pips. Panel B draws the "regular" quotes, i.e. the best bid and ask price good for up to 50 mio.

around 1 or 2 pips, becomes highly volatile and reaches levels in excess of 100 pips in the midst of the sell-off.[24] Panel B plots the "regular" quote (i.e. the best bid and offer available for a fixed amount of 50 mio) over the same period and from here it is clear that the book is very sparse over the sell-off and that the ability to quickly trade out of large positions was severely impaired. Both these observations highlight that while price continuity was preserved over this episode of extreme volatility, liquidity on the other hand severely deteriorated. This is a point also recently emphasized in O'Hara (2010) and we believe it indicates an important avenue for future research.

[24]It is interesting to note that the spread also turns substantially negative at times. In the OTC FX market (where counterparties need to provide credit to each other) a negative spread can be observed if the participant that aggresses the market does not have credit against the counterparties providing liquidity at the top of book. Over the sell-off, several participants were forced to pay for liquidity by hitting deep into the opposite side of the orderbook reflecting their lack of credit. So in this instance, a large spread of either sign can indicate market turbulence. On a centrally cleared market one would not expect to see this behavior.

References

Aït-Sahalia, Y., 2004, "Disentangling diffusion from jumps," *Journal of Financial Economics*, 74(3), 487–528.

Aït-Sahalia, Y., and J. Jacod, 2009a, "Analyzing the spectrum of asset returns: Jump and volatility components in high frequency data," Working paper, Princeton University.

———, 2009b, "Estimating the degree of activity of jumps in high frequency data," *Annals of Statistics*, 37(5), 2202–2244.

———, 2009c, "Testing for jumps in a discretely observed process," *Annals of Statistics*, 37(1), 184–222.

Aït-Sahalia, Y., P. A. Mykland, and L. Zhang, 2005, "How often to sample a continuous-time process in the presence of market microstructure noise," *Review of Financial Studies*, 18(2), 351–416.

Andersen, T. G., L. Benzoni, and J. Lund, 2002, "An empirical investigation of continuous-time equity return models," *Journal of Finance*, 57(4), 1239–1284.

Andersen, T. G., T. Bollerslev, and F. X. Diebold, 2007, "Roughing it up: Including jump components in the measurement, modeling and forecasting of return volatility," *Review of Economics and Statistics*, 89(4), 701–720.

———, 2010, "Parametric and nonparametric volatility measurement," in *Handbook of Financial Econometrics*, ed. by L. P. Hansen, and Y. Ait-Sahalia. North-Holland, pp. 67–138.

Andersen, T. G., T. Bollerslev, F. X. Diebold, and P. Labys, 2003, "Modeling and forecasting realized volatility," *Econometrica*, 71(2), 579–625.

Andersen, T. G., T. Bollerslev, and X. Huang, 2011, "A reduced form framework for modeling volatility of speculative prices based on realized variation measures," *Journal of Econometrics*, 160(1), 176–189.

Andersen, T. G., D. Dobrev, and E. Schaumburg, 2008, "Jump robust volatility estimation using nearest neighbour truncation," Working paper, Northwestern University.

———, 2010, "Integrated quarticity estimation: Theory and practical implementation," Working paper, Northwestern University.

Back, K., 1991, "Asset prices for general processes," *Journal of Mathematical Economics*, 20(4), 371–395.

Bakshi, G. S., C. Cao, and Z. Chen, 1997, "Empirical performance of alternative option pricing models," *Journal of Finance*, 52(2), 2003–2049.

Bakshi, G. S., and G. Panayotov, 2010, "First-passage probability, jump models, and intra-horizon risk," *Journal of Financial Economics*, 95(1), 20–40.

Ball, C. A., and W. N. Torous, 1983, "A simplified jump process for common stock returns," *Journal of Financial and Quantitative Analysis*, 18(1), 53–65.

———, 1985, "On jumps in common stock prices and their impact on call option pricing," *Journal of Finance*, 40(1), 155–173.

Bandi, F. M., and J. R. Russell, 2006, "Separating microstructure noise from volatility," *Journal of Financial Economics*, 79(3), 655–692.

Barndorff-Nielsen, O. E., S. E. Graversen, J. Jacod, M. Podolskij, and N. Shephard, 2006, "A central limit theorem for realized power and bipower variations of continuous semimartingales," in *From Stochastic Calculus to Mathematical Finance: The Shiryaev Festschrift*, ed. by Y. Kabanov, R. Lipster, and J. Stoyanov. Springer-Verlag, pp. 33–68.

Barndorff-Nielsen, O. E., P. R. Hansen, A. Lunde, and N. Shephard, 2008, "Designing realised kernels to measure the ex-post variation of equity prices in the presence of noise," *Econometrica*, 76(6), 1481–1536.

———, 2009, "Realized kernels in practice: trades and quotes," *Econometrics Journal*, 12(3), 1–32.

Barndorff-Nielsen, O. E., and N. Shephard, 2004, "Power and bipower variation with stochastic volatility and jumps," *Journal of Financial Econometrics*, 2(1), 1–48.

———, 2006, "Econometrics of testing for jumps in financial economics using bipower variation," *Journal of Financial Econometrics*, 4(1), 1–30.

———, 2007, "Variation, jumps, market frictions and high frequency data in financial econometrics," in *Advances in Economics and Econometrics: Theory and Applications, Ninth World Congress*, ed. by R. Blundell, P. Torsten, and W. K. Newey. Cambridge University Press.

Barndorff-Nielsen, O. E., N. Shephard, and M. Winkel, 2006, "Limit theorems for multipower variation in the presence of jumps," *Stochastic Processes and their Applications*, 116(5), 796–806.

Bates, D. S., 1996, "Jumps and stochastic volatility: Exchange rate processes implicit in Deutsche Mark options," *Review of Financial Studies*, 9(1), 69–107.

———, 2000, "Post-'87 crash fears in the S&P500 futures option market," *Journal of Econometrics*, 94, 181–238.

———, 2006, "Maximum likelihood estimation of latent affine processes," *Review of Financial Studies*, 19(3), 909–965.

———, 2011, "U.S. stock market crash risk, 1926 - 2010," Working paper, University of Iowa.

Beckers, S., 1981, "A note on estimating the parameters of the diffusion-jump model of stock returns," *Journal of Financial and Quantitative Analysis*, 16(1), 127–140.

Black, F., 1976, "Studies of stock market volatility changes," in *Proceedings of the American Statistical Association*, pp. 177–181. Business and Economic Statistics Section.

———, 1986, "Noise," *Journal of Finance*, 41(3), 529–543.

Bollerslev, T., U. Kretschmer, C. Pigorsch, and G. Tauchen, 2009, "A discrete-time model for daily S&P500 returns and realized variations: jumps and leverage effects," *Journal of Econometrics*, 150(2), 151–166.

Bollerslev, T., T. H. Law, and G. Tauchen, 2008, "Risk, jumps, and diversification," *Journal of Econometrics*, 144(1), 234–256.

Bollerslev, T., and H. Zhou, 2002, "Estimating stochastic volatility diffusion using conditional moments of integrated volatility," *Journal of Econometrics*, 109(1), 33–65.

Chernov, M., A. R. Gallant, E. Ghysels, and G. Tauchen, 2003, "Alternative models for stock price dynamics," *Journal of Econometrics*, 116(1-2), 225–257.

Christensen, K., R. C. A. Oomen, and M. Podolskij, 2010, "Realised quantile-based estimation of the integrated variance," *Journal of Econometrics*, 159(1), 74–98.

Christie, A. A., 1982, "The stochastic behavior of common stock variances: Value, leverage and interest rate effects," *Journal of Financial Economics*, 10(4), 407–432.

Corsi, F., D. Pirino, and R. Renò, 2010, "Threshold bipower variation and the impact of jumps on volatility forecasting," *Journal of Econometrics*, 159(2), 276–288.

Corsi, F., and R. Renò, 2009, "Volatility determinants: Heterogeneity, leverage, and jumps," Working paper, available at http://ssrn.com/abstract=1316953.

Cox, J. C., and S. A. Ross, 1976, "The valuation of options for alternative stochastic processes," *Journal of Financial Economics*, 3(1-2), 145–166.

Delbaen, F., and W. Schachermayer, 1994, "A general version of the fundamental theorem of asset pricing," *Mathematische Annalen*, 300, 463–520.

Diebold, F. X., and G. H. Strasser, 2008, "On the correlation structure of microstructure noise in theory and practice," Working paper, University of Pennsylvania.

Duffie, D., and J. Pan, 2001, "Analytical Value-at-Risk with jumps and credit risk," *Finance and Stochastics*, 5, 155–180.

Duffie, D., J. Pan, and K. J. Singleton, 2000, "Transform analysis and asset pricing for affine jump-diffusions," *Econometrica*, 68(6), 1343–1376.

Easley, D., M. M. L. de Prado, and M. O'Hara, 2011, "The microstructure of the flash crash: Flow toxicity, liquidity crashes and the probability of informed trading," *Journal of Portfolio Management*, 37(2), 118–128.

Eraker, B., 2004, "Do stock prices and volatility jump? Reconciling evidence from spot and option prices," *Journal of Finance*, 59(3), 1367–1403.

Eraker, B., M. Johannes, and N. Polson, 2003, "The impact of jumps in volatility and returns," *Journal of Finance*, 58(3), 1269–1300.

Fama, E. F., 1965, "The behavior of stock-market prices," *Journal of Business*, 38(1), 34–105.

Gatheral, J., and R. C. A. Oomen, 2010, "Zero-intelligence realized variance estimation," *Finance and Stochastics*, 14(2), 249–283.

Gloter, A., and J. Jacod, 2001a, "Diffusions with measurement errors. I - local asymptotic normality," *ESAIM: Probability and Statistics*, 5, 225–242.

———, 2001b, "Diffusions with measurement errors. II - measurement errors," *ESAIM: Probability and Statistics*, 5, 243–260.

Hansen, P. R., and A. Lunde, 2006, "Realized variance and market microstructure noise," *Journal of Business and Economic Statistics*, 24(2), 127–161.

Hautsch, N., and M. Podolskij, 2010, "Pre-averaging based estimation of quadratic variation in the presence of noise and jumps: Theory, implementation, and empirical evidence," Working paper, Humboldt-Universität zu Berlin.

Huang, X., and G. Tauchen, 2005, "The relative contribution of jumps to total price variance," *Journal of Financial Econometrics*, 3(4), 456–499.

Jacod, J., 2008, "Statistics and high frequency data," Lecture notes.

Jacod, J., Y. Li, P. A. Mykland, M. Podolskij, and M. Vetter, 2009, "Microstructure noise in the continuous case: The pre-averaging approach," *Stochastic Processes and their Applications*, 119(7), 2249–2276.

Jacod, J., M. Podolskij, and M. Vetter, 2010, "Limit theorems for moving averages of discretized processes plus noise," *Annals of Statistics*, 38(3), 1478–1545.

Jarrow, R. A., and E. R. Rosenfeld, 1984, "Jump risks and the intertemporal capital asset pricing model," *Journal of Business*, 57(3), 337–351.

Jiang, G. J., and R. C. A. Oomen, 2007, "Estimating latent variables and jump diffusion models using high-frequency data," *Journal of Financial Econometrics*, 5(1), 1–30.

Johannes, M., 2004, "The statistical and economic role of jumps in continuous-time interest rate models," *Journal of Finance*, 59(1), 227–260.

Jorion, P., 1988, "On jump processes in the foreign exchange and stock markets," *Review of Financial Studies*, 1(4), 427–445.

Kalnina, I., 2011, "Subsampling high frequency data," *Journal of Econometrics*, 161(2), 262–283.

Kirilenko, A. A., A. S. Kyle, M. Samadi, and T. Tuzun, 2011, "The flash crash: The impact of high frequency trading on an electronic market," Working paper, available at ssrn.com/abstract=1686004.

Liu, J., F. Longstaff, and J. Pan, 2003, "Dynamic asset allocation with event risk," *Journal of Finance*, 58(1), 231–259.

Maheu, J. M., and T. H. McCurdy, 2004, "News arrival, jump dynamics, and volatility components for individual stock returns," *Journal of Finance*, 59(2), 755–793.

Mancini, C., 2004, "Estimation of the characteristics of jump of a general Poisson-diffusion model," *Scandinavian Actuarial Journal*, 2004(1), 42–52.

———, 2009, "Non parametric threshold estimation for models with stochastic diffusion coefficient and jumps," *Scandinavian Journal of Statistics*, 36(2), 270–296.

Mandelbrot, B. B., 1963, "The variation of certain speculative prices," *Journal of Business*, 36(4), 394–419.

Merton, R. C., 1976, "Option pricing when underlying stock returns are discontinuous," *Journal of Financial Economics*, 3(1-2), 125–144.

Mykland, P. A., N. Shephard, and K. Sheppard, 2010, "Econometric analysis of financial jumps using efficient bipower variation," Working paper, Oxford-Man Institute, University of Oxford.

Niederhoffer, V., and M. F. M. Osborne, 1966, "Market making and reversal on the stock exchange," *Journal of the American Statistical Association*, 61(316), 897–916.

O'Hara, M., 2010, "What is a quote?," *Journal of Trading*, 5(2), 10–16.

Oomen, R. C. A., 2006, "Comment on 2005 JBES invited address "Realized variance and market microstructure noise" by Peter R. Hansen and Asger Lunde," *Journal of Business and Economic Statistics*, 24(2), 195 – 202.

Pan, J., 2002, "The jump-risk premia implicit in options: Evidence from an integrated time-series study," *Journal of Financial Economics*, 63(1), 3–50.

Patton, A. J., and K. Sheppard, 2011, "Good volatility, bad volatility: Signed jumps and the persistence of volatility," Working paper, Duke University.

Podolskij, M., and M. Vetter, 2009a, "Bipower-type estimation in a noisy diffusion setting," *Stochastic Processes and their Applications*, 119(9), 2803–2831.

———, 2009b, "Estimation of volatility functionals in the simultaneous presence of microstructure noise and jumps," *Bernoulli*, 15(3), 634–658.

Press, S. J., 1967, "A compound events model for security prices," *Journal of Business*, 40(3), 317–335.

Protter, P. E., 2004, *Stochastic Integration and Differential Equations*. Springer-Verlag, 1 edn.

Roll, R., 1984, "A simple implicit measure of the effective bid-ask spread in an efficient market," *Journal of Finance*, 39(4), 1127–1139.

Tauchen, G., and H. Zhou, 2011, "Realized jumps on financial markets and predicting credit spreads," *Journal of Econometrics*, 160(1), 102–118.

Todorov, V., 2009, "Estimation of continuous-time stochastic volatility models with jumps using high-frequency data," *Journal of Econometrics*, 148(2), 131–148.

Zhang, L., 2006, "Efficient estimation of stochastic volatility using noisy observations: A multi-scale approach," *Bernoulli*, 12(6), 1019–1043.

Zhang, L., P. A. Mykland, and Y. Aït-Sahalia, 2005, "A tale of two time scales: determining integrated volatility with noisy high-frequency data," *Journal of the American Statistical Association*, 100(472), 1394–1411.

Zhou, B., 1996, "High-frequency data and volatility in foreign-exchange rates," *Journal of Business and Economic Statistics*, 14(1), 45–52.

A Finite sample bias in bipower variation

In a simple model, it is possible to work out an approximate expression for the finite sample bias in the BV defined by Eq. (7) in the main text in the paper. To this end, consider the model

$$X_t = \int_0^t \sigma_s \mathrm{d}W_s,$$

where $\sigma \perp\!\!\!\perp W$. Moreover, we assume that the variance process σ^2 is bounded away from 0 and has the form

$$\sigma_t^2 = \sigma_0^2 + \int_0^t \eta_s \mathrm{d}s + \int_0^t \upsilon_s \mathrm{d}B_s,$$

where B is another Brownian motion with $B \perp\!\!\!\perp W$. Let

$$BV_N[X] = \frac{1}{\mu^2} \sum_{i=2}^{N} |\Delta_{i-1}^N X||\Delta_i^N X|.$$

Here, we initially leave out the correction $N/(N-1)$ used to define BV in the main text. We add it back later.

Then, the conditional bias of $BV_N[X]$ is given as

$$E\left(BV_N[X] - \int_0^1 \sigma_s^2 \mathrm{d}s \mid \sigma\right) = \sum_{i=1}^{N-1} \left\{ \left(\int_{\frac{i-1}{N}}^{\frac{i}{N}} \sigma_s^2 \mathrm{d}s \right)^{1/2} \left(\int_{\frac{i}{N}}^{\frac{i+1}{N}} \sigma_s^2 \mathrm{d}s \right)^{1/2} - \int_{\frac{i-1}{N}}^{\frac{i}{N}} \sigma_s^2 \mathrm{d}s \right\} - \int_{\frac{N-1}{N}}^{1} \sigma_s^2 \mathrm{d}s$$

To simplify notation, we define $f(x) = \sqrt{x}$ and set

$$a_i = N \int_{\frac{i-1}{N}}^{\frac{i}{N}} \sigma_s^2 \mathrm{d}s.$$

Hence,

$$E\left(BV_N[X] - \int_0^1 \sigma_s^2 \mathrm{d}s \mid \sigma\right) = \frac{1}{N}\left(a_N + \sum_{i=1}^{N-1} f(a_i)(f(a_{i+1}) - f(a_i)) \right).$$

By Burkholder's inequality, we get

$$E(|a_{i+1} - a_i|^p) \leq C N^{-p/2}$$

for any $p > 0$. Thus,

$$E\left(BV_N[X] - \int_0^1 \sigma_s^2 \mathrm{d}s \mid \sigma\right) = \frac{1}{N}\left(a_N + \sum_{i=1}^{N-1} f(a_i)\{f'(a_i)(a_{i+1} - a_i) + \frac{f''(a_i)}{2}(a_{i+1} - a_i)^2\} \right) + o_p(N^{-1}).$$

Note that $f'(x) = \frac{1}{2}x^{-1/2}$ and $f''(x) = -\frac{1}{4}x^{-3/2}$. Using this, we deduce that

$$\frac{1}{N} \sum_{i=1}^{N-1} f(a_i) f'(a_i)(a_{i+1} - a_i) = \frac{1}{2N}(a_N - a_1) = \frac{1}{2N}(\sigma_1^2 - \sigma_0^2) + o_p(N^{-1}).$$

On the other hand,

$$\frac{1}{N}\sum_{i=1}^{N-1} f(a_i)\frac{f''(a_i)}{2}(a_{i+1}-a_i)^2 = -\frac{1}{N}\sum_{i=1}^{N-1}\frac{1}{8}\frac{(a_{i+1}-a_i)^2}{a_i}.$$

Because σ^2 is a continuous semimartingale, a standard approximation scheme yields

$$-\frac{1}{N}\sum_{i=1}^{N-1}\frac{1}{8}\frac{(a_{i+1}-a_i)^2}{a_i} = -N\sum_{i=1}^{N-1}\frac{1}{8}\frac{\upsilon^2_{\frac{i-1}{N}}}{\sigma^2_{\frac{i-1}{N}}}\left(\int_{\frac{i}{N}}^{\frac{i+1}{N}} B_s\mathrm{d}s - \int_{\frac{i-1}{N}}^{\frac{i}{N}} B_s\mathrm{d}s\right)^2 + o_p(N^{-1}).$$

Moreover, as

$$E\left(\left[\int_{\frac{i}{N}}^{\frac{i+1}{N}} B_s\mathrm{d}s - \int_{\frac{i-1}{N}}^{\frac{i}{N}} B_s\mathrm{d}s\right]^2\right) = \frac{2}{3N^3},$$

we conclude that

$$-\frac{1}{N}\sum_{i=1}^{N-1}\frac{1}{8}\frac{(a_{i+1}-a_i)^2}{a_i} = -\frac{1}{N}\frac{1}{12}\int_0^1 \frac{\upsilon_s^2}{\sigma_s^2}\mathrm{d}s + o_p(N^{-1}).$$

Putting everything together, we find that

$$E\left(BV_N[X] - \int_0^1 \sigma_s^2\mathrm{d}s \mid \sigma\right) = -\frac{1}{N}\left(\frac{1}{12}\int_0^1 \frac{\upsilon_s^2}{\sigma_s^2}\mathrm{d}s + \frac{1}{2}(\sigma_1^2+\sigma_0^2)\right) + o_p(N^{-1}).$$

Now, applying the finite sample correction $N/(N-1)$ cancels out the effect of the "missing" summand and adds an additional $\int_0^1 \sigma_s^2\mathrm{d}s/N$ term to the conditional bias:

$$E\left(\frac{N}{N-1}BV_N[X] - \int_0^1 \sigma_s^2\mathrm{d}s \mid \sigma\right) = -\frac{1}{N}\left(\frac{1}{12}\int_0^1 \frac{\upsilon_s^2}{\sigma_s^2}\mathrm{d}s + \frac{1}{2}(\sigma_1^2+\sigma_0^2) - \int_0^1 \sigma_s^2\mathrm{d}s\right) + o_p(N^{-1}).$$

Note that this expression is not negative in general, but that the sign and magnitude of the dependence on υ are unaffected by the adjustment. Finally, taking unconditional expectations and assuming that σ^2 is a stationary process, we find that

$$E\left(\frac{N}{N-1}BV_N[X] - \int_0^1 \sigma_s^2\mathrm{d}s\right) = -\frac{1}{N}E\left(\frac{1}{12}\int_0^1 \frac{\upsilon_s^2}{\sigma_s^2}\mathrm{d}s\right) + o(N^{-1}).$$

This is the expression given in the main text, which is negative up to terms of order $o(N^{-1})$.

B The explicit form of Σ^*

In the main text, we proposed a consistent estimator of the asymptotic covariance matrix appearing in Proposition 1, Σ^*, without giving the exact form of Σ^*. Here, a formula for it is provided. We set $f_i : \mathbb{R}^2 \to \mathbb{R}$, $i = 1, 2$, equal to

$$f_1(x) = x_1^2, \qquad f_2(x) = \frac{|x_1||x_2|}{\mu^2}.$$

Then, for $x \in \mathbb{R}$, $u \in [0,1]$ and $l = -1, \ldots, 2$, we define

$$F^{(ij)}_{l,x,u} = \mathrm{cov}(f_i(S), f_j(T)) \qquad 1 \le i, j \le 2,$$

where $S = (S_1, S_2)'$, $T = (T_1, T_2)'$ are centered and jointly normal with

(i) $S_i \perp S_j$, $T_i \perp T_j$ for all $i \neq j$.

(ii) $\text{var}(S_i) = \text{var}(T_i) = \theta\psi_2 x^2 + \frac{\psi_1}{\theta}\omega^2$ for all i.

(iii) $\text{cov}(S_{i+l-1}, T_i) = \theta w_g(u) x^2 + \frac{1}{\theta} w_{g'}(u)\omega^2$ for all i.

(iv) $\text{cov}(S_{i+l}, T_i) = \theta w_g(1-u) x^2 + \frac{1}{\theta} w_{g'}(1-u)\omega^2$ for all i.

(v) $\text{cov}(S_i, T_j) = 0$ for all $|i + l - j - 1| > 1$.

Here, the function $w_g(u)$ is given by

$$w_g(u) = \int_0^{1-u} g(y)\, g(y+u)\, \mathrm{d}y.$$

Finally, we get that

$$\Sigma^* = \frac{1}{\theta\psi_2^2} \sum_{l=-1}^{2} \int_0^1 \int_0^1 F_{l,\sigma_s,u} \mathrm{d}s \mathrm{d}u.$$

C The definition of QRV in the absence of noise

As a starter, we should note that the QRV can be defined on either raw or absolute returns, see Christensen, Oomen, and Podolskij (2010) for details. In this paper, we base the QRV on absolute returns, which fits nicely into the extant literature on realised variation.

Let

$$D_{i,m} Y = \left(\Delta_k^N Y\right)_{i \leq k \leq i+m-1},$$

for $i \geq 1$. Moreover, we define the quantile function $g_k : \mathbb{R}^m \to \mathbb{R}$ such that

$$g_k(x) = x_{(k)},$$

where $x_{(k)}$ is the kth order statistic of $x = (x_1, \ldots, x_m)$.

Then, the (subsampled) QRV based on absolute returns is defined as

$$QRV_N[Y] \equiv \alpha' QRV_N(m, \overline{\lambda}),$$

where $\bar{\lambda} = (\lambda_1, \ldots, \lambda_k)$ with $\lambda_j \in [0, 1)$ is a vector of quantiles, $\lambda_j m$ is a natural number for all j, $\alpha = (\alpha_1, \ldots, \alpha_k)$ with $\alpha_j \geq 0$ and $\sum_{j=1}^k \alpha_j = 1$ are quantile weights, and the jth element of $QRV_N(m, \overline{\lambda})$ is given by:

$$QRV_N(m, \lambda_j) = \frac{1}{N-m} \sum_{i=1}^{N-m} \frac{q_i(m, \lambda_j)}{\nu_1(m, \lambda_j)},$$

for $j = 1, \ldots, k$, where

$$q_i(m,\lambda) = g^2_{\lambda m}\left(\sqrt{N}|D_{i,m}Y|\right) \qquad \text{and} \qquad \nu_r\left(m,\lambda\right) = \mathbb{E}\left[\left(|U|_{(\lambda m)}\right)^{2r}\right].$$

D Appendix of proofs

Proof of Proposition 2 Here, we only show the convergence in probability of the estimator $\hat{\Sigma}^*_{11}$. The consistency of the other matrix entries ($\hat{\Sigma}^*_{12}$ and $\hat{\Sigma}^*_{22}$) can be proved in exactly the same way. Also, in this part of the proof, we assume that the process X is continuous. Later, we add jumps back and show that the limit is unchanged.

It should be spelled out that, if X is continuous,

$$RV^*_N[Y] - \int_0^1 \sigma^2_s \mathrm{d}s = O_p(N^{-1/4}),$$

see Proposition 1. Hence, it implies that $\int_0^1 \sigma^2_s \mathrm{d}s$ can be replaced by $RV^*_N[Y]$ in the definition of $\hat{\Sigma}^*_{11}$ without affecting its limit.

As a first step, we note that due to a standard localization technique, we can assume that the processes a and σ are bounded. Moreover, as has been shown in Jacod, Li, Mykland, Podolskij, and Vetter (2009), the following approximations hold (uniformly in m):

$$RV^*_{N,m}[Y] = \frac{d}{K\psi^K_2}\sum_{j=0}^{[(N/L-m+1)/d]}\left(\sum_{i=0}^{L-K}|\sigma_{\frac{(m-1+jd)L}{N}}\bar{W}^N_i + \bar{u}^N_i|^2\right) - \frac{\psi^K_1}{\theta^2\psi^K_2}\omega^2 + o_p(1),$$

$$\int_0^1 \sigma^2_s \mathrm{d}s = \frac{dL}{N}\sum_{j=0}^{[(N/L-m+1)/d]}\sigma^2_{\frac{(m-1+jd)L}{N}} + o_p(1).$$

Setting

$$\chi^N_{j,m} = \sum_{i=0}^{L-K}|\sigma_{\frac{(m-1+jd)L}{N}}\bar{W}^N_i + \bar{u}^N_i|^2,$$

we deduce that

$$RV^*_{N,m}[Y] - \int_0^1 \sigma^2_s \mathrm{d}s = \frac{d}{K\psi_2}\sum_{j=0}^{[(N/L-m+1)/d]}\left(\chi^N_{j,m} - E[\chi^N_{j,m}|\mathcal{F}_{\frac{(m-1+jd)L}{N}}]\right) + o_p(1).$$

This yields the decomposition

$$\hat{\Sigma}^*_{11} = \frac{1}{d}\sum_{m=1}^{d}\left(\frac{N^{1/4}}{d^{1/2}}\left(RV^*_{N,m}[Y] - \int_0^1 \sigma^2_s \mathrm{d}s\right)\right)^2 = V_n + R_n + o_p(1),$$

with

$$V_n = \frac{N^{1/2}}{K^2\psi_2^2}\sum_{m=1}^{d}\sum_{j=0}^{[(N/L-m+1)/d]}\Big(\chi_{j,m}^N - E[\chi_{j,m}^N|\mathcal{F}_{\frac{(m-1+jd)L}{N}}]\Big)^2,$$

$$R_n = \frac{2N^{1/2}}{K^2\psi_2^2}\sum_{m=1}^{d}\sum_{j_1\neq j_2}\Big(\chi_{j_1,m}^N - E[\chi_{j_1,m}^N|\mathcal{F}_{\frac{(m-1+j_1d)L}{N}}]\Big)\Big(\chi_{j_2,m}^N - E[\chi_{j_2,m}^N|\mathcal{F}_{\frac{(m-1+j_2d)L}{N}}]\Big).$$

By relying on the results of Jacod, Li, Mykland, Podolskij, and Vetter (2009), we already know that

$$V_n \xrightarrow{p} \Sigma_{11}^*.$$

Thus, all that is left to prove is that $R_n \xrightarrow{p} 0$.

We start by noting that the summands in the definition of R_n are mutually uncorrelated for all m, j_1, j_2. Moreover, the terms $\chi_{j_1,m}^N - E[\chi_{j_1,m}^N|\mathcal{F}_{\frac{(m-1+j_1d)L}{N}}]$ and $\chi_{j_2,m}^N - E[\chi_{j_2,m}^N|\mathcal{F}_{\frac{(m-1+j_2d)L}{N}}]$ are also uncorrelated for $j_1 \neq j_2$. Appealing again to Jacod, Li, Mykland, Podolskij, and Vetter (2009), it holds that

$$E[|\sigma_{\frac{(m-1+jd)L}{N}}\bar{W}_i^N + \bar{u}_i^N|^4] \leq \frac{C}{N},$$

if $E(u^4) < \infty$. In addition, the terms $|\sigma_{\frac{(m-1+jd)L}{N}}\bar{W}_{i_1}^N + \bar{u}_{i_1}^N|^2$ and $|\sigma_{\frac{(m-1+jd)L}{N}}\bar{W}_{i_2}^N + \bar{u}_{i_2}^N|^2$ are uncorrelated for $|i_1 - i_2| > K$, which taken together implies that

$$E[|\chi_{j,m}^N|^2] \leq C\frac{KL}{N}$$

for all m and j. Finally, some straightforward calculations show that

$$\text{var}(R_n) = \frac{4N}{K^4\psi_2^4}\sum_{m=1}^{d}\sum_{j_1\neq j_2}E\Big(\chi_{j_1,m}^N - E[\chi_{j_1,m}^N|\mathcal{F}_{\frac{(m-1+j_1d)L}{N}}]\Big)^2 E\Big(\chi_{j_2,m}^N - E[\chi_{j_2,m}^N|\mathcal{F}_{\frac{(m-1+j_2d)L}{N}}]\Big)^2 \leq C\frac{N}{dK^2}.$$

As $K = O(\sqrt{N})$ and $d \to \infty$, we thus find that

$$R_n \xrightarrow{p} 0,$$

which completes the proof of Proposition 2, if X is continuous.

To finish the proof, we now consider the general case, where X possesses finite-activity jumps. In this situation, the subsampled estimators $RV_{N,m}^*[Y]$ are affected by jumps only for finitely many m's (due to finite-activity of the jump part). From Jacod, Podolskij, and Vetter (2010), it follows that

$$RV_{N,m}^*[Y] - \int_0^1 \sigma_s^2 \mathrm{d}s = O_p(1),$$

if $RV^*_{N,m}[Y]$ is affected by jumps for a given m. Thus, we conclude that

$$\hat{\Sigma}^*_{11} = \frac{1}{d}\sum_{m=1}^{d}\left(\frac{N^{1/4}}{d^{1/2}}\left(RV^*_{N,m}[Z] - \int_0^1 \sigma_s^2 \mathrm{d}s\right)\right)^2 + O_p(\sqrt{N}/d^2),$$

where $Z = X^c + u$ and X^c denotes the continuous part of X. But $\sqrt{N}/d^2 \to 0$, and so we are done. ■

Proof of Proposition 3 To show that the results of Proposition 1 are robust to the presence of outliers, as we model it by Eq. (30), we first recall that the definition in Eq. (31) implies that there are only finitely many i's such that $O_{i/N} \neq 0$. Here, we confine attention to proving the outlier robustness of the $RV^*_N[Y]$ estimator. The robustness property of $BV^*_N[Y]$ can be proved using almost identical tools.

Thus, recall that

$$RV^*_N[Y] = \frac{N}{N-K+2}\frac{1}{K\psi_2^K}\sum_{i=0}^{N-K+1}|\bar{Y}_i^N|^2 - \frac{\psi_1^K}{\theta^2\psi_2^K}\hat{\omega}^2_{\text{AC}},$$

where

$$\hat{\omega}^2_{\text{AC}} = -\frac{1}{N-1}\sum_{i=2}^{N}\Delta_{i-1}^N Y \Delta_i^N Y.$$

To show that $\hat{\omega}^2_{\text{AC}}$ is robust to outliers ($\hat{\omega}^2_{\text{AC}}$ can be replaced by the estimator $\hat{\omega}^2_{\text{RV}}$ defined in the main text without altering the validity of the proof), we note that

$$\hat{\omega}^2_{\text{AC}} = -\frac{1}{N-1}\sum_{i=2}^{N}\Delta_{i-1}^N u \Delta_i^N u + O_p(N^{-1}).$$

So, in particular, $\hat{\omega}^2_{\text{AC}}$ is robust to the presence of finite-activity outliers. In the next step, we know that with probability converging to one any interval of the form $[i/N, (i+K)/N]$ contains at most a single outlier. Moreover, by expressing $\bar{Y}_i^N$ via an identity using log-prices, it follows that

$$\bar{Y}_i^N = \sum_{j=1}^{K}\Big[g\Big(\frac{j-1}{K}\Big) - g\Big(\frac{j}{K}\Big)\Big]Y_{(i+j-1)/N},$$

where it is used that $g(0) = g(1) = 0$. Hence, an outlier $O_{l/N}$ in $[i/N, (i+K)/N]$ induces a bias of the form $\Big[g\Big(\frac{l-i}{K}\Big) - g\Big(\frac{l-i+1}{K}\Big)\Big]O_{l/N}$ and, as there are finitely many outliers, only $O(K)$ of the pre-averaging returns $\bar{Y}_i^N$ are affected by these. Thus, by putting the parts together, we conclude that

$$\frac{N}{N-K+2}\frac{1}{K\psi_2^K}\sum_{i=0}^{N-K+1}|\bar{Y}_i^N|^2 = \frac{N}{N-K+2}\frac{1}{K\psi_2^K}\sum_{i=0}^{N-K+1}|\bar{Z}_i^N|^2 + O_p(K^{-1}),$$

where $Z = X + u$. Thus, the law of large numbers and CLT for RV^*_N are robust to the presence of outliers. ■

Proof of Theorem 1 We are dealing with finitely many jumps and outliers in the data, and they never appear together, because $N^J \perp\!\!\!\perp N^O$. Thus, with probability approaching one, we observe at most a single jump or outlier (and not both) on any interval of the form $[i/N, (i+m)/N]$ with m fixed.

Take $QRV_N[Y]$ first. If a jump appears on some interval $[i/N, (i+m)/N]$, it affects one return of Y, which will asymptotically dominate all other returns (in absolute value) on $[i/N, (i+m)/N]$, because the rest originate from the continuous part of Y. Meanwhile, if an outlier appears on the interval $[i/N, (i+m)/N]$, it affects two consecutive returns of Y, and they again asymptotically dominate all other returns on $[i/N, (i+m)/N]$. The condition $\max(\lambda_j) < 1 - 1/m$ then ensures that those dominating terms are not taken into account, when computing the $QRV_N[Y]$, i.e. this estimator is robust to the presence of jumps and outliers:

$$QRV_N[Y] \xrightarrow{p} \int_0^1 \sigma_s^2 \mathrm{d}s.$$

Next, $BV_N[Y]$ is well-known to be robust against jumps (Barndorff-Nielsen and Shephard, 2004). To figure out the influence of outliers on this estimator, we decompile it into two components

$$BV_N[Y] = \frac{N}{N-1}\frac{1}{\mu^2}\Big(\sum_{i \in B_N} |\Delta_{i-1}^N Y||\Delta_i^N Y| + \sum_{i \in B_N^c} |\Delta_{i-1}^N Y||\Delta_i^N Y| \Big)$$

with $B_N = \{i \mid O_{i/N} \neq 0\}$. It readily follows that

$$BV_N[Y] \xrightarrow{p} \int_0^1 \sigma_s^2 \mathrm{d}s + \frac{1}{\mu^2} \sum_{i=1}^{N_1^O} \mathcal{S}_i^2.$$

Last but not least, we decompose $RV_N[Y]$ into three parts

$$RV_N[Y] = \sum_{i \in (\bar{A}_N \cup \bar{B}_N)^c} |\Delta_i^N Y|^2 + \sum_{i \in \bar{A}_N} |\Delta_i^N Y|^2 + \sum_{i \in \bar{B}_N} |\Delta_i^N Y|^2,$$

where $\bar{A}_N = \{i \mid X \text{ jumps on } [(i-1)/N, i/N]\}$ and $\bar{B}_N = \{i \mid O_{(i-1)/N} \neq 0 \text{ or } O_{i/N} \neq 0\}$. Note that the sets $\bar{A}_N$ and $\bar{B}_N$ are asymptotically disjoint, as $N^J \perp\!\!\!\perp N^O$. Again, this readily implies that

$$RV_N[Y] \xrightarrow{p} \int_0^1 \sigma_s^2 \mathrm{d}s + \sum_{i=1}^{N_1^J} J_i^2 + 2 \sum_{i=1}^{N_1^O} \mathcal{S}_i^2$$

and the proof is complete. ■

Proof of Theorem 2 The stable CLT for $(RV_N[Y], BV_N[Y])$ has been shown in Barndorff-Nielsen, Graversen, Jacod, Podolskij, and Shephard (2006), while the corresponding result for $QRV_N[Y]$ has been proved in Christensen, Oomen,

and Podolskij (2010). Here, we show a joint CLT for the vector $(RV_N[Y], BV_N[Y], QRV_N[Y])$ via Theorem 7.1 from Jacod (2008).

We define

$$V(f)_N = \sum_{i=1}^{N} f(\sqrt{N}\Delta_i^N Y, \ldots, \sqrt{N}\Delta_{i+m-1}^N Y),$$

where $f = (f_1, f_2, f_3) : \mathbb{R}^m \to \mathbb{R}^3$ is given by

$$f_1(x) = x_1^2, \qquad f_2(x) = \frac{|x_1||x_2|}{\mu^2}, \qquad f_3(x) = \frac{|x|_{(m\lambda)}^2}{\nu_1(m,\lambda)}$$

with $x = (x_1, \ldots, x_m)$. Then, for any $y \in \mathbb{R}$, we set

$$\rho_y(f) = E[f(yU_1, \ldots, yU_m)] \in \mathbb{R}^3, \qquad (U_1, \ldots, U_m) \sim N_m(0, I_m).$$

This gives us the identity

$$N^{1/2}\begin{pmatrix} RV_N[Y] - \int_0^1 \sigma_s^2 \mathrm{d}s \\ BV_N[Y] - \int_0^1 \sigma_s^2 \mathrm{d}s \\ QRV_N[Y] - \int_0^1 \sigma_s^2 \mathrm{d}s \end{pmatrix} = N^{1/2}\bigg(N^{-1}V(f)_N - \int_0^1 \rho_{\sigma_s}(f)\mathrm{d}s\bigg).$$

Applying Theorem 7.1 in Jacod (2008), we deduce that

$$N^{1/2}\bigg(N^{-1}V(f)_N - \int_0^1 \rho_{\sigma_s}(f)\mathrm{d}s\bigg) \xrightarrow{d_s} MN\bigg(0, \int_0^1 R_{\sigma_s}(f)\mathrm{d}s\bigg),$$

where $R_y(f) = (R_y^{jk}(f))_{1\leq j,k\leq 3}$ is defined by

$$R_y^{jk}(f) = \sum_{l=-m+1}^{m-1} E[f_j(yU_m, \ldots, yU_{2m-1}) f_k(yU_{l+m}, \ldots, yU_{l+2m-1})]$$

$$- (2m-1)E[f_j(yU_1, \ldots, yU_m)]E[f_k(yU_1, \ldots, yU_m)],$$

where $(U_i)_{1\leq i\leq m}$ are i.i.d. $N(0,1)$.[25] Finally, a simple computation shows that

$$\int_0^1 R_{\sigma_s}(f)\mathrm{d}s = \int_0^1 \sigma_s^4 \mathrm{d}s \times \Sigma,$$

where the matrix Σ is given in Theorem 2. This completes the proof. ■

[25] Strictly speaking, Theorem 7.1 in Jacod (2008) cannot be applied directly, because the functions f_2 and f_3 are not everywhere differentiable. However, the problem of non-differentiability was solved in Barndorff-Nielsen, Graversen, Jacod, Podolskij, and Shephard (2006) for the function f_2 and in Christensen, Oomen, and Podolskij (2010) for the function f_3.

Research Papers
2011

2011-05: Michael Sørensen: Prediction-based estimating functions: review and new developments

2011-06: Søren Johansen: An extension of cointegration to fractional autoregressive processes

2011-07: Tom Engsted and Stig V. Møller: Cross-sectional consumption-based asset pricing: The importance of consumption timing and the inclusion of severe crises

2011-08: Tommaso Proietti and Stefano Grassi: Bayesian stochastic model specification search for seasonal and calendar effects

2011-09: Matt P. Dziubinski: Option valuation with the simplified component GARCH model

2011-10: Tim A. Kroencke, Felix Schindler and Andreas Schrimpf: International Diversification Benefits with Foreign Exchange Investment Styles

2011-11: Eduardo Rossi and Paolo Santucci de Magistris: Estimation of long memory in integrated variance

2011-12: Matias D. Cattaneo, Richard K. Crump and Michael Jansson: Generalized Jackknife Estimators of Weighted Average Derivatives

2011-13: Dennis Kristensen: Nonparametric Detection and Estimation of Structural Change

2011-14: Stefano Grassi and Paolo Santucci de Magistris: When Long Memory Meets the Kalman Filter: A Comparative Study

2011-15: Antonio E. Noriega and Daniel Ventosa-Santaularia: A Simple Test for Spurious Regressions

2011-16: Stefano Grassi and Tommaso Proietti: Characterizing economic trends by Bayesian stochastic model specification search

2011-17: Søren Johansen and Theis Lange: Some econometric results for the Blanchard-Watson bubble model

2011-18: Tom Engsted and Thomas Q. Pedersen: Bias-correction in vector autoregressive models: A simulation study

2011-19: Kim Christensen, Roel Oomen and Mark Podolskij: Fact or friction: Jumps at ultra high frequency